

Phase Field Modeling of Diffusion-Controlled Defect Processes

(Wang and Li, Acta Mater, Overview 150, 2010)

Yunzhi Wang

Department of Materials Science and Engineering
The Ohio State University

Acknowledgement

N. Zhou and M.J. Mills – OSU

C. Shen - GE Global Research

J. Li -Penn

ONR/DARPA, AFOSR and NSF/DOE

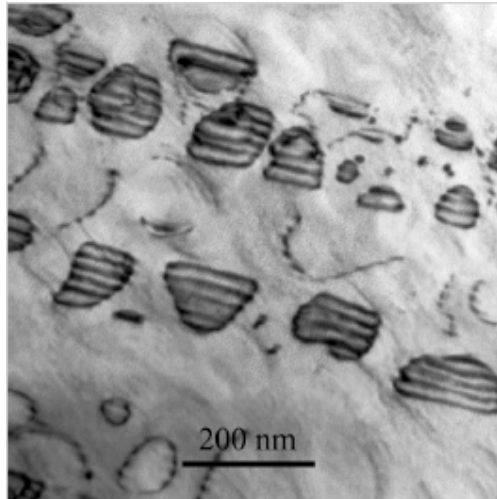
NIST Diffusion Workshop, March 23-24, 2010



Outline

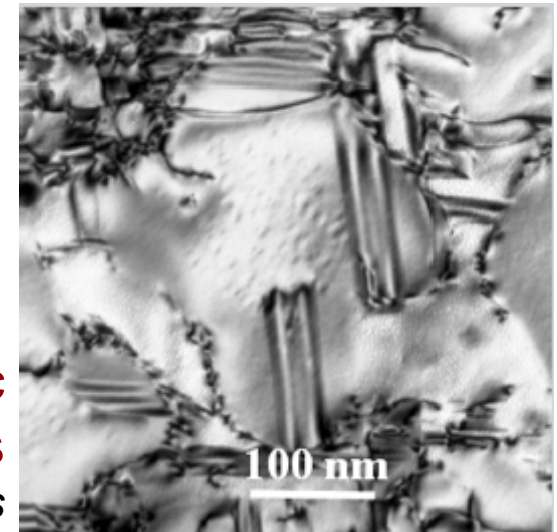
- Mechano-chemical coupling and diffusion-controlled defect processes – experimental observations
- Phase field description of defects
- Traditional coarse-grained phase field method
- Microscopic phase field method
- Diffusional molecular dynamics (DMD) method
- Integrated phase field modeling
- Conclusions

A cornucopia of deformation mechanisms in superalloys



Superlattice Extrinsic Stacking Faults

- Milligan and Antolovich
- Chen and Knowles
- Viswanathan



Superlattice Intrinsic Stacking Faults

- Chen and Knowles

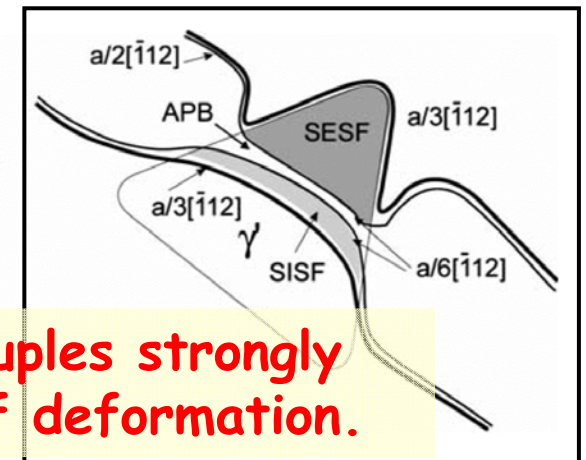


Stacking Fault Ribbons

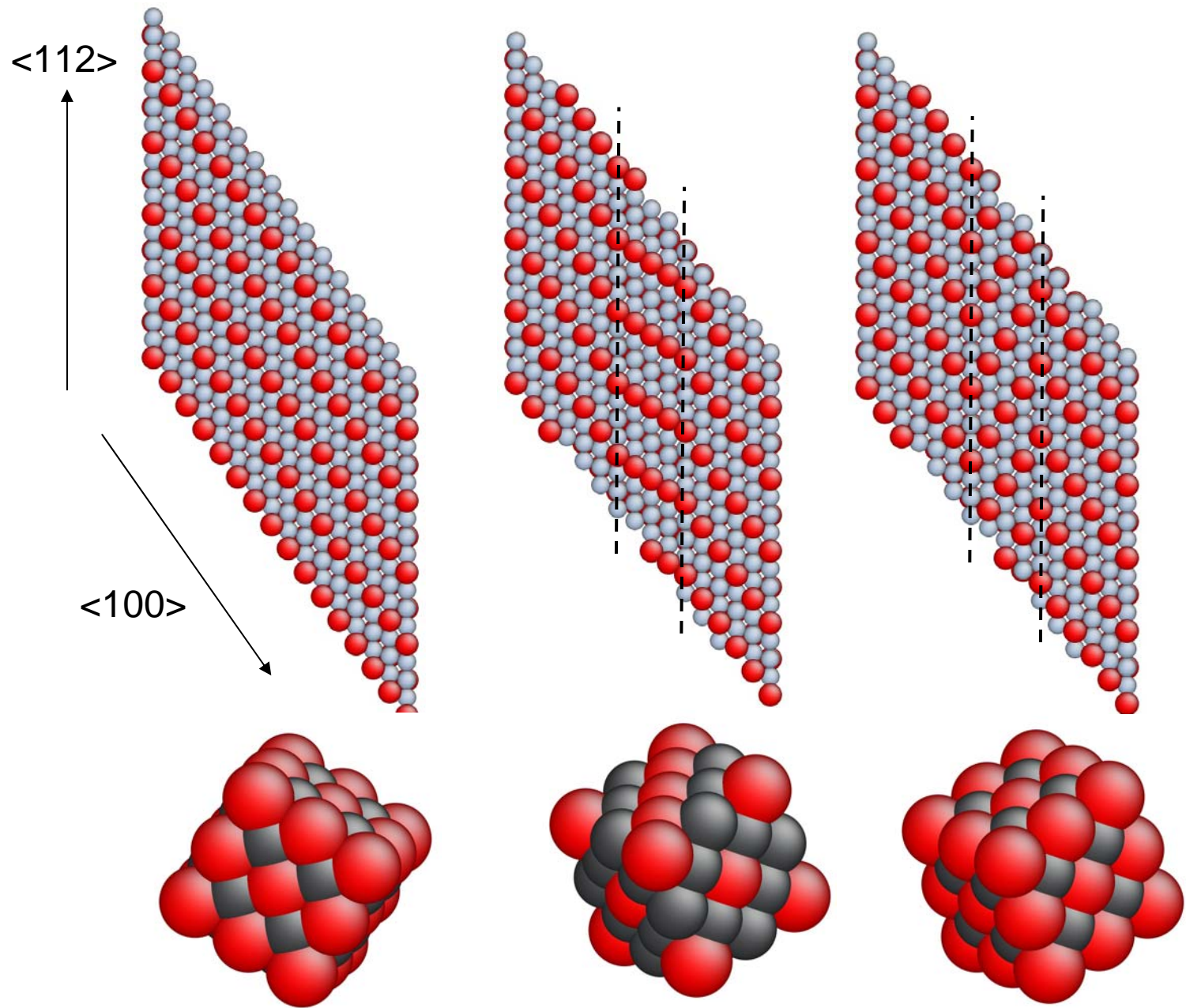
- Kear & Oblack
- Rae and Reed

Microtwinning

- Kear
- Ardakani, Mclean & Shollock
- Chen and Knowles
- Viswanathan



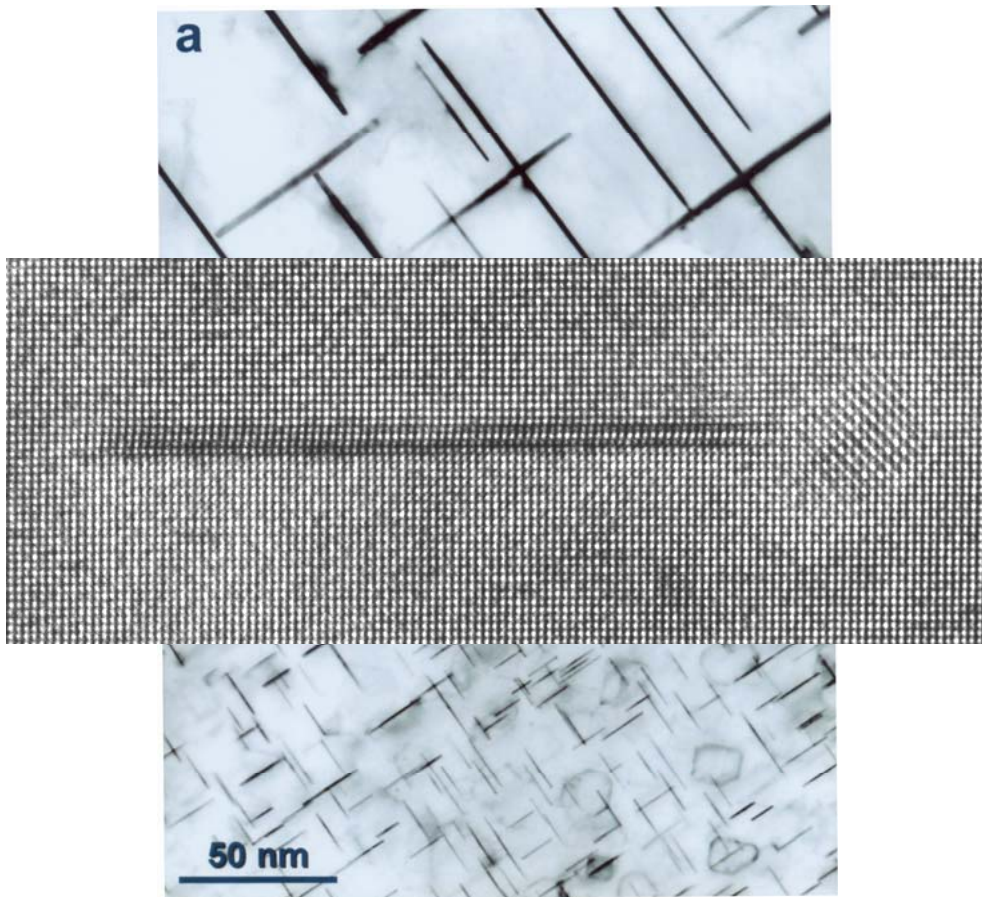
In all these processes, chemical reordering couples strongly to dislocation shearing in governing the rate of deformation.



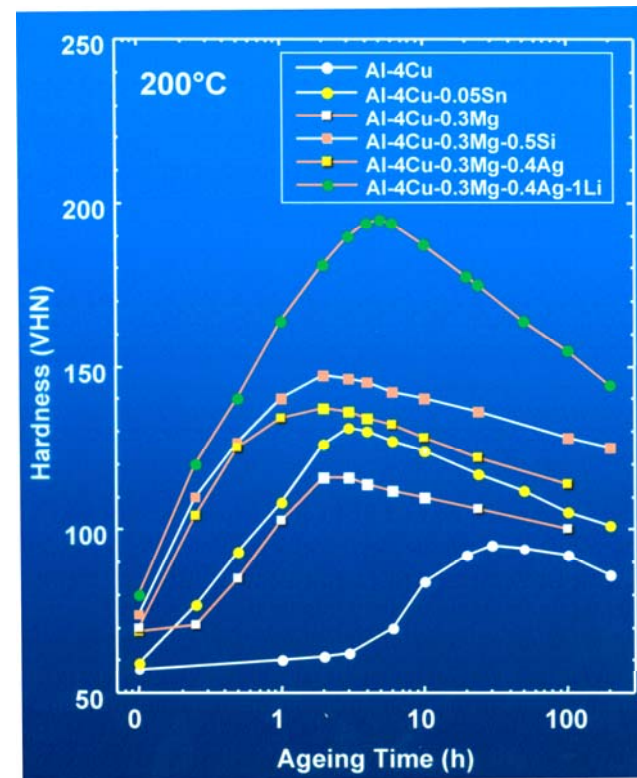
(a) Untwinned

(b) Pseudo Twin

(c) True Twin

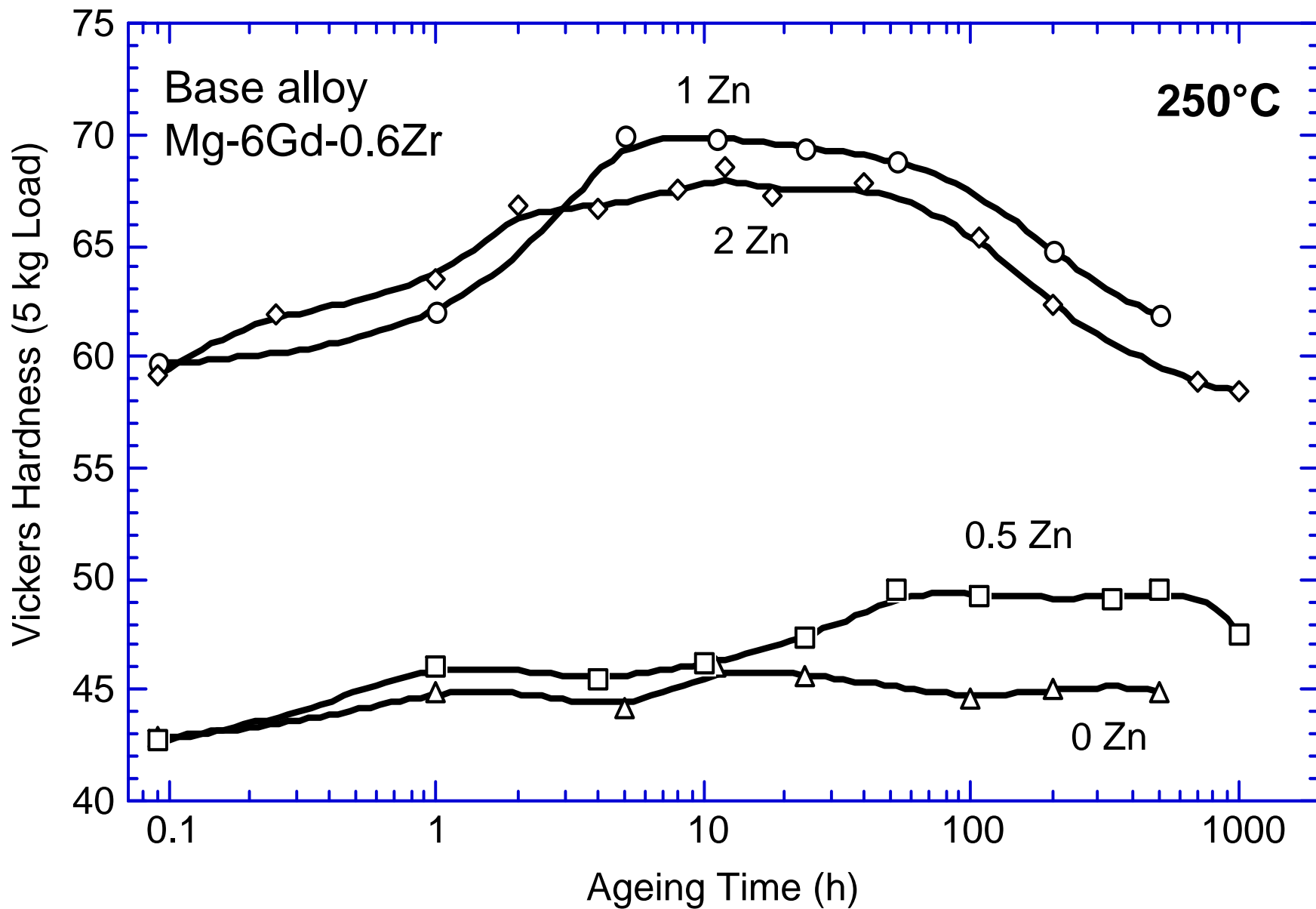


(a) Al-4Cu, and (b) Al-4Cu-0.05Sn
190°C/18h

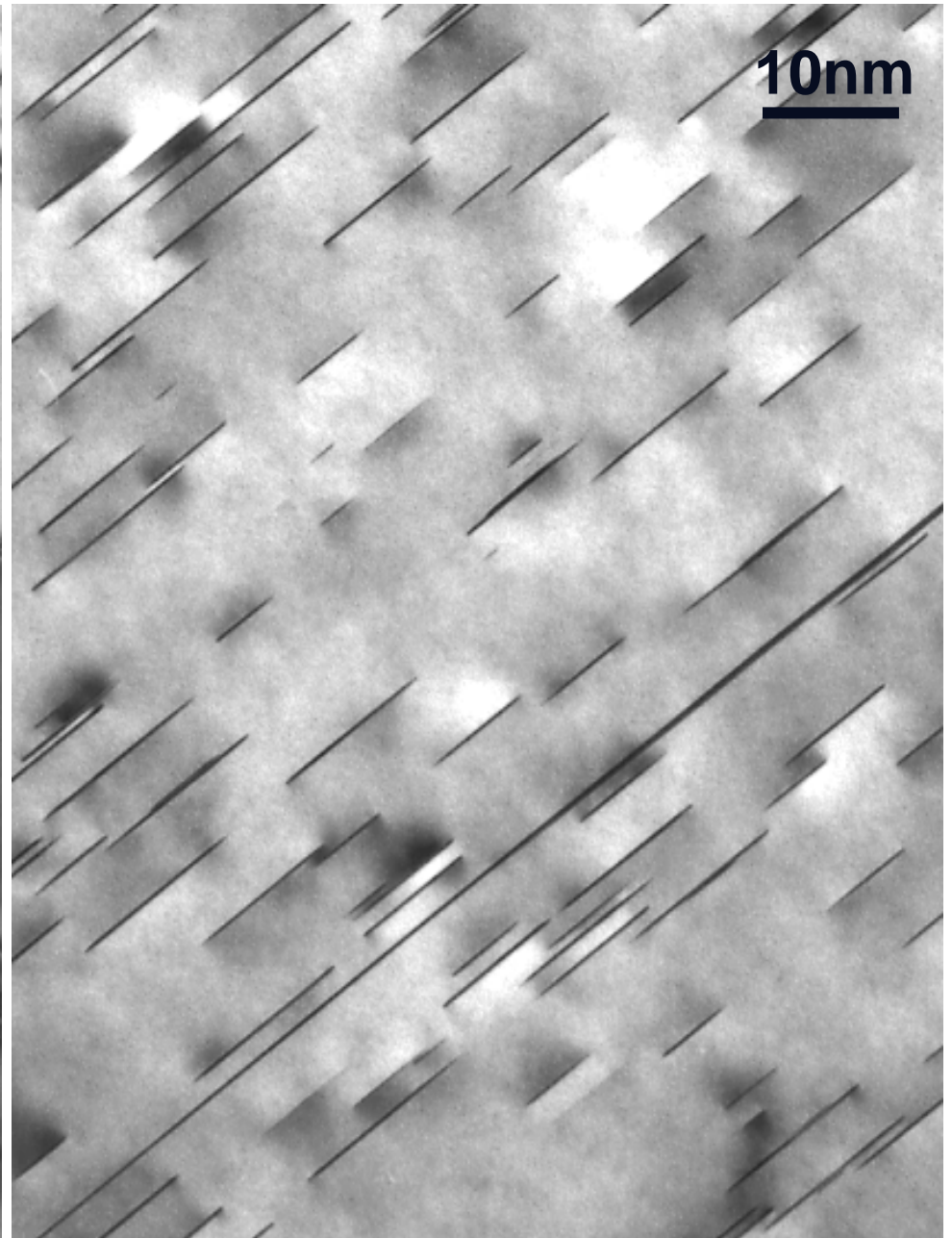
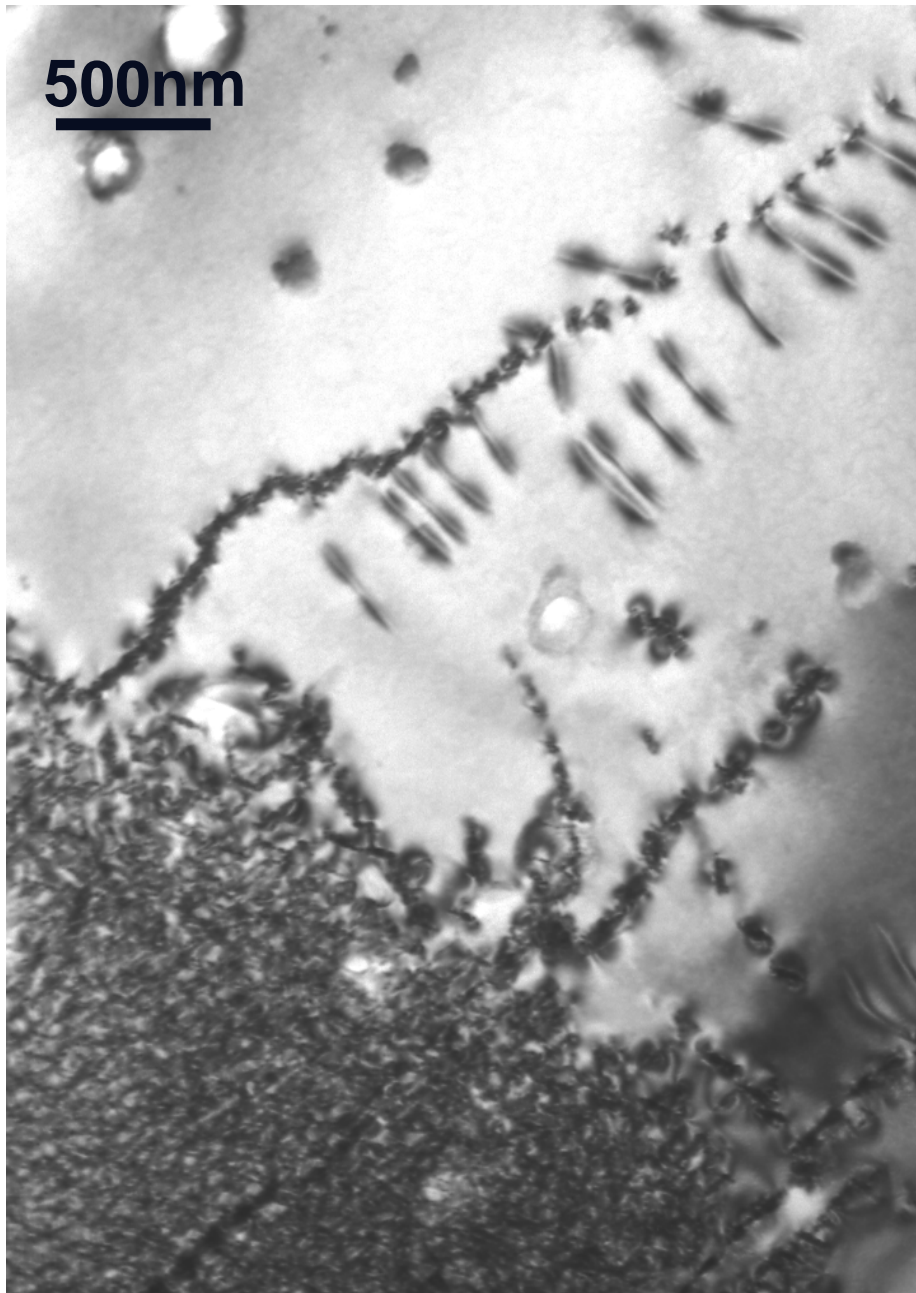


(Courtesy of B.C. Muddle and J.F. Nie)

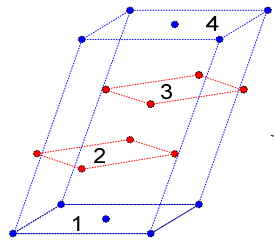




Nie, Gao and Zhu, Scripta Mater. 2005



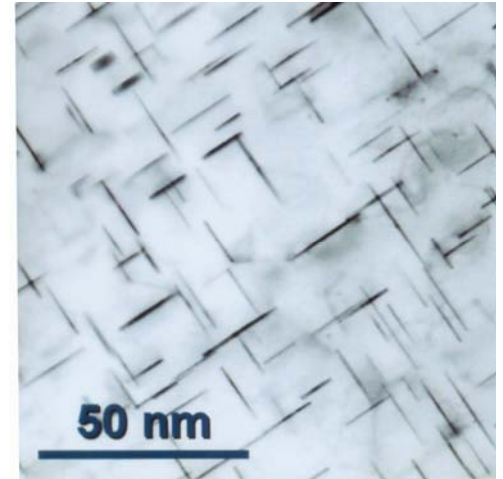
Possible transformation mechanism for θ' precipitation



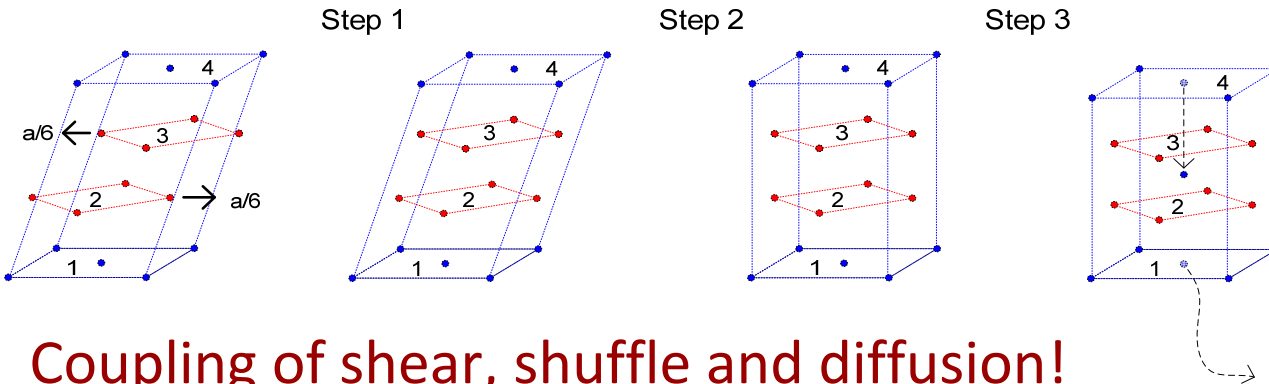
- 1) "Shifts" of layers 2 and 3 in opposite direction by $a/6$ vector
- 2) Homogeneous shear of whole cell by the angle $\arctan(1/3)$
- 3) Shuffle of Cu atom to the centre of the cell, and diffusion of the other Cu atom away to the matrix

MEP

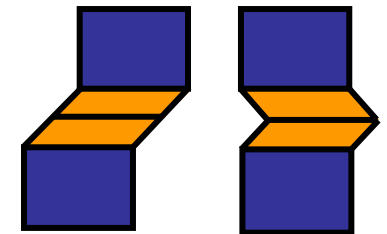
(Nie and Muddle)



Al-4Cu-0.5Sn



Coupling of shear, shuffle and diffusion!

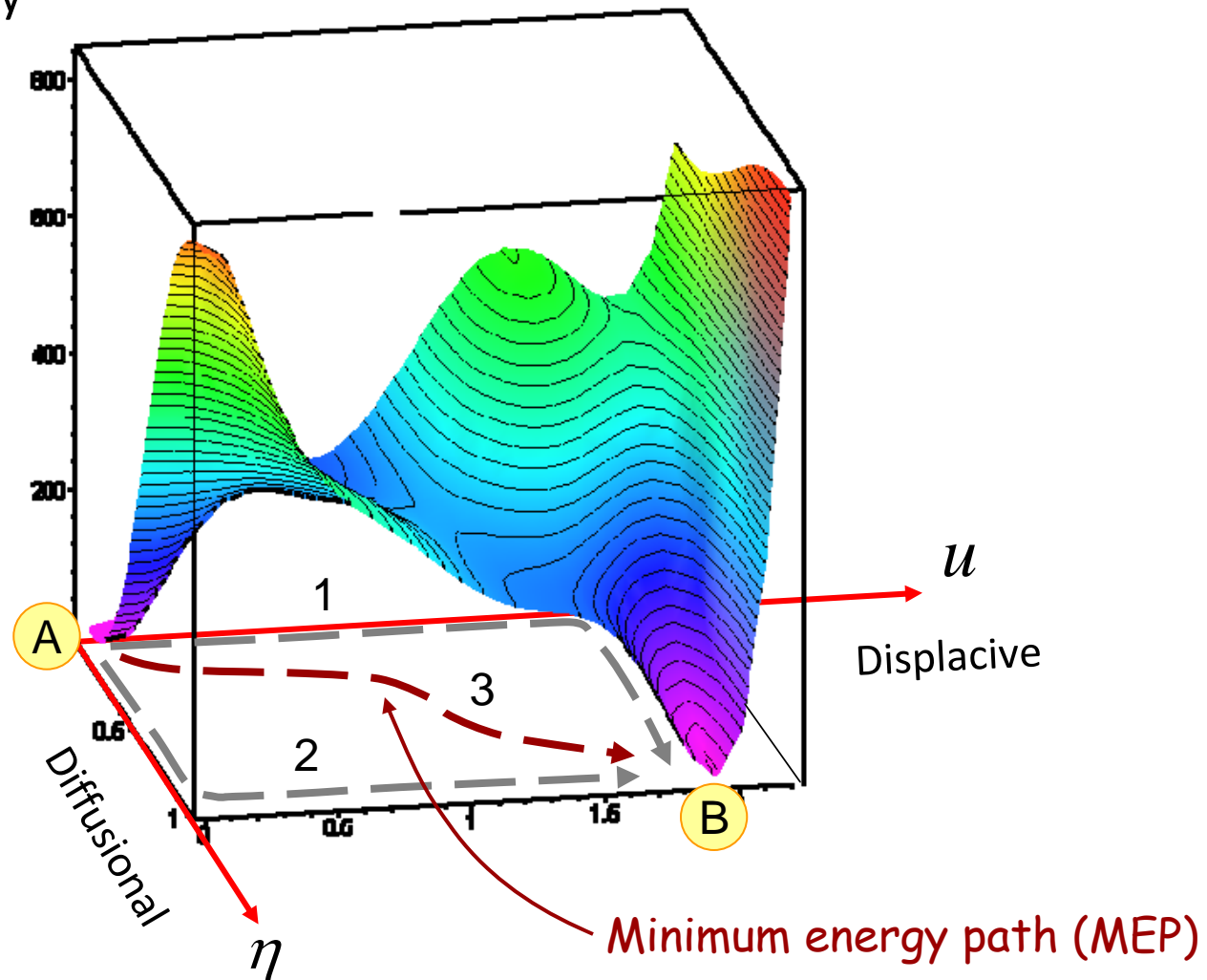


Accommodation of shape strain plays a key role

Alloy	Precipitate Phase	Habit Plane
Al-Cu	θ' (Al_2Cu)	$\{100\}_\alpha$
Al-Cu-Mg-Ag	Ω (Al_2Cu)	$\{111\}_\alpha$
Al-Cu-Li(-Mg-Ag)	T_1 (Al_2CuLi)	$\{111\}_\alpha$
Al-Zn-Mg(-Cu)	η' ($MgZn_2$)	$\{111\}_\alpha$

Chemical – mechanical coupling

Total energy landscape



Challenges

Key problem

Mechano-chemical coupling and diffusion-controlled defect processes

Atomistic methods

Empirical potential MD: accuracy limited by available atomic potentials

Direct *ab initio* MD: simulation limited to ~300 atoms

*Time scale limit: ~30 years of atomistic simulations of dislocations, all people did was glide!

kMC: even-catalogs may be difficult to generate

Continuum methods

Peierls-Nabarro type models: use *ab initio* GSF energy as input, but limited to dislocative process of simple defect geometry

DDD, coarse-grained PFM and others: defect structure, energy and mobility, and mechanisms are model input rather than output

Phase field description of defects

Order parameter $\phi(\mathbf{r})$

Chemical non-uniformity: $c(\mathbf{r}), \rho(\mathbf{r}), V_m(\mathbf{r}), \dots$

Structural non-uniformity: $\eta(\mathbf{r}), \mathbf{u}(\mathbf{r}), \boldsymbol{\varepsilon}(\mathbf{r}), \mathbf{M}(\mathbf{r}),$

Total energy

Chemical or inelastic energy:

$$F^{ch} = \int [f(\phi(\mathbf{r})) + \kappa |\nabla \phi(\mathbf{r})|^2] d\mathbf{r}$$

Elastic energy: $\varepsilon_{ij}^T(\mathbf{r}) = \sum_p \varepsilon_{ij}^T(\phi_p(\mathbf{r}))$

$$E^{el} = \frac{1}{2} \sum_{pq} \int \frac{d^3k}{(2\pi)^3} \begin{bmatrix} C_{ijkl} \varepsilon_{ij}^{00}(p) \varepsilon_{kl}^{00}(q) \\ -n_i \sigma_{ij}^{00}(p) \Omega_{jk}(\mathbf{n}) \sigma_{kl}^{00}(q) n_l \end{bmatrix} \{\phi_p^m(\mathbf{r})\}_k \{\phi_q^m(\mathbf{r})\}_k^*$$

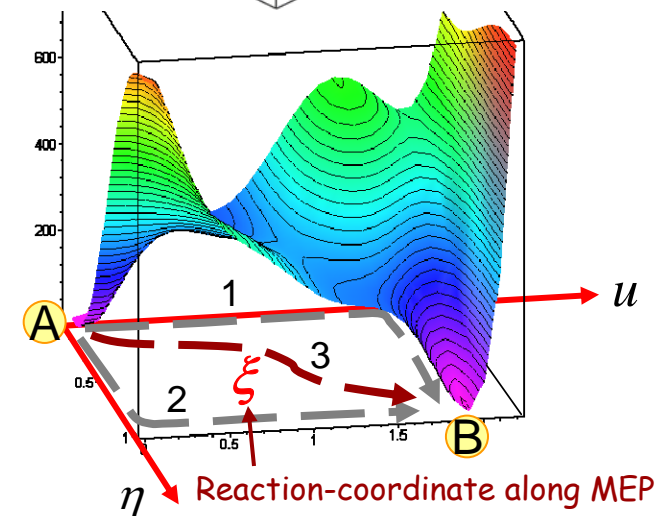
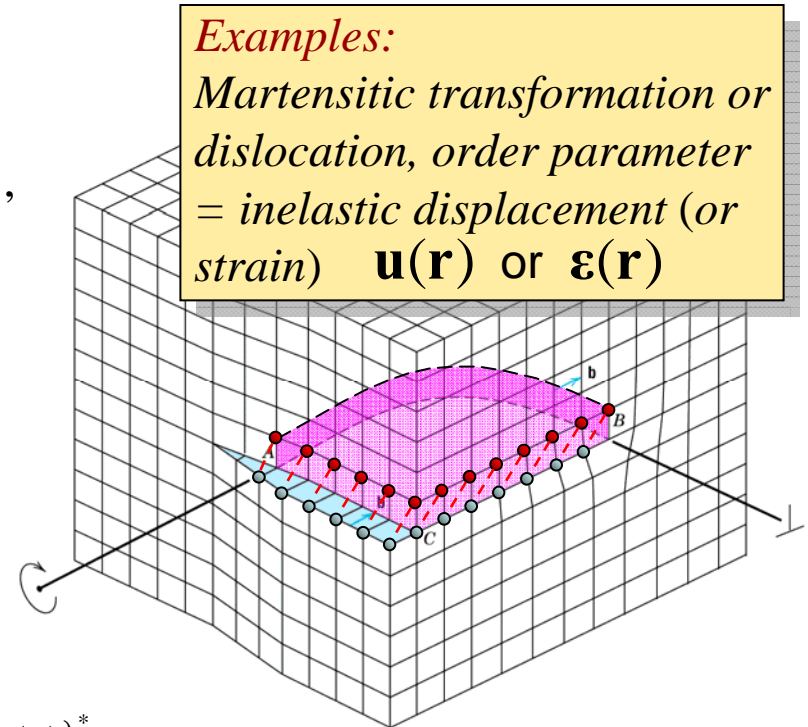
Kinetics

$$\frac{\partial \phi(\mathbf{r}, t)}{\partial t} = -\hat{\mathbf{M}} \frac{\delta F}{\delta \phi(\mathbf{r}, t)} + \xi(\mathbf{r}, t)$$

$$\hat{\mathbf{M}} = \begin{cases} M & \text{for non-conserved order parameter} \\ -M \nabla^2 & \text{for conserved order parameter} \end{cases}$$

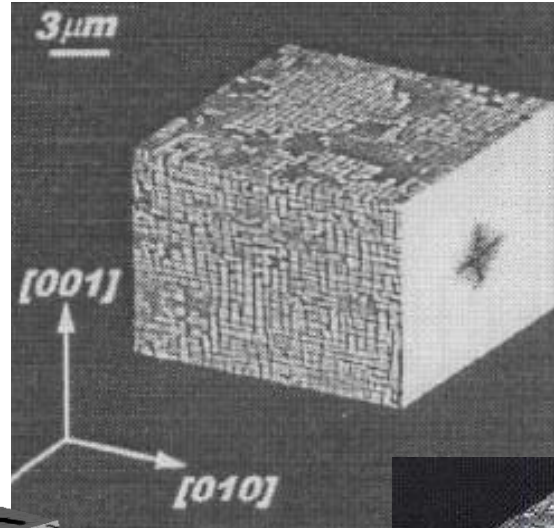
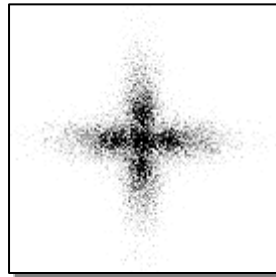
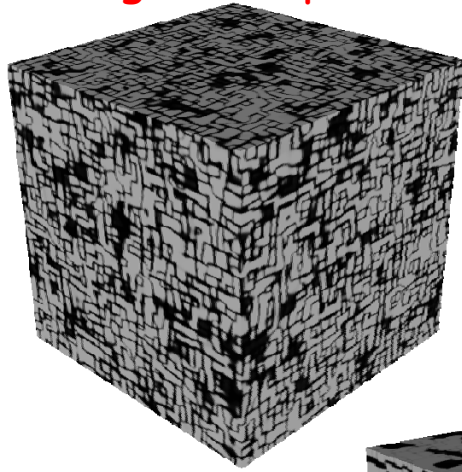
Examples:

Martensitic transformation or dislocation, order parameter = inelastic displacement (or strain) $\mathbf{u}(\mathbf{r})$ or $\boldsymbol{\varepsilon}(\mathbf{r})$

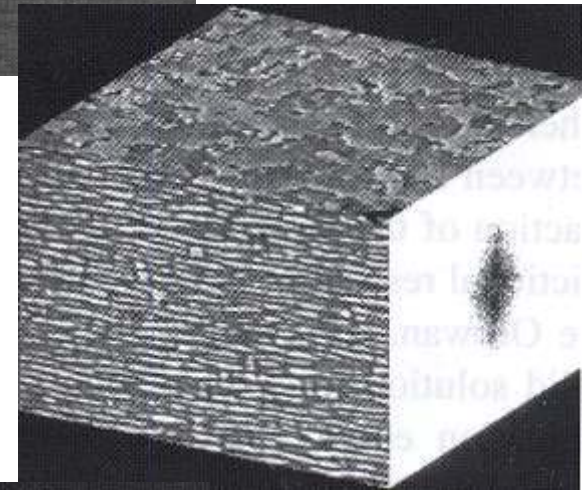
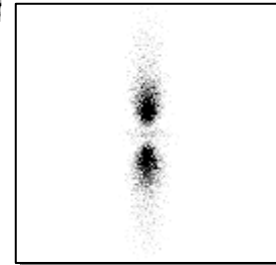
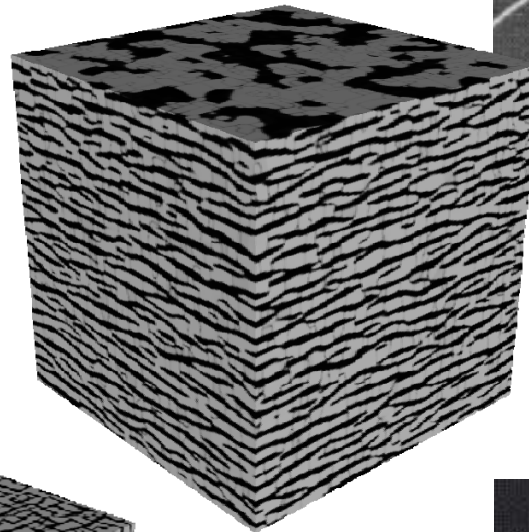


Coarse-grained phase field simulations

Experimental observations



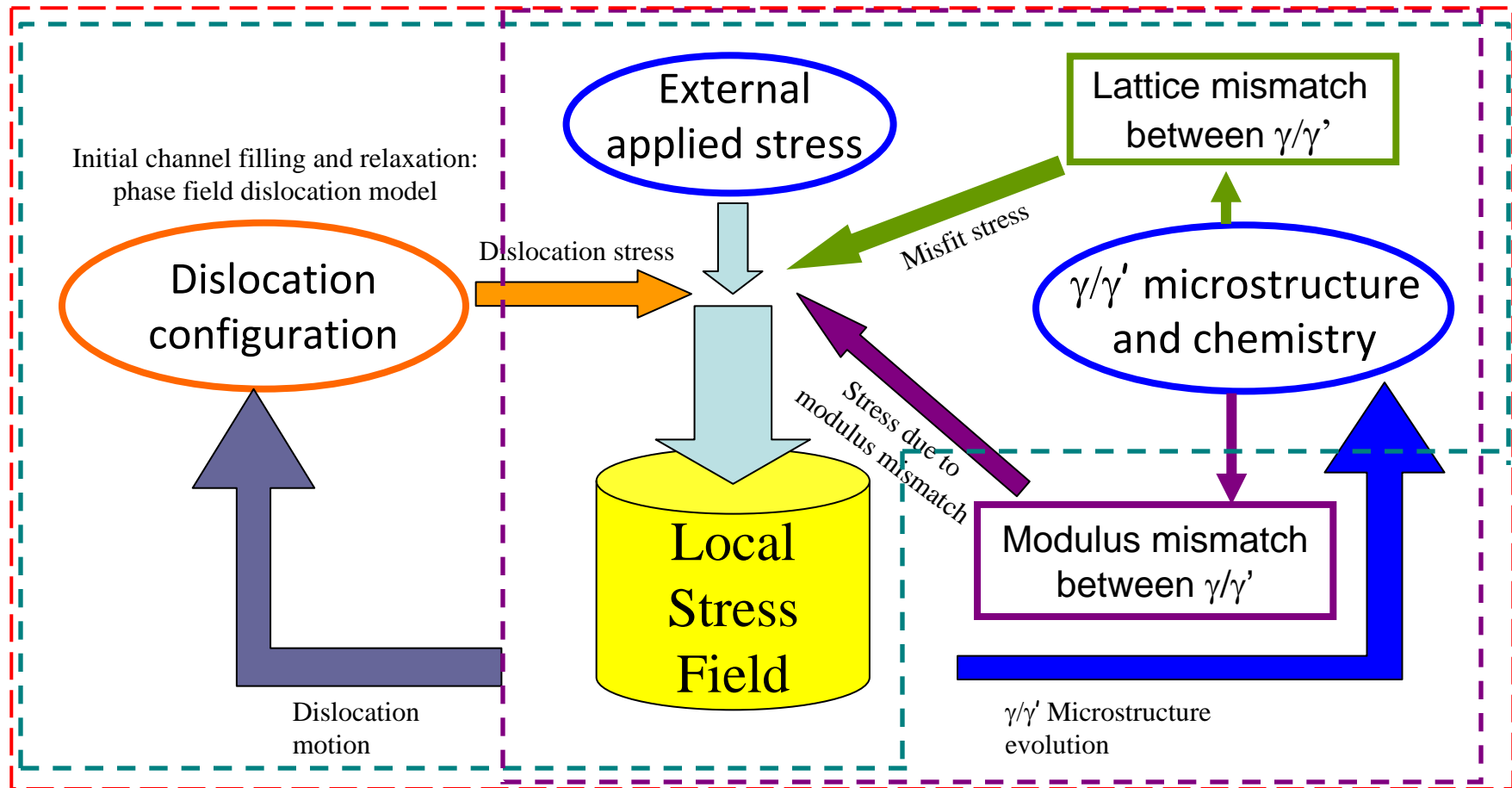
N. Zhou, C. Shen, M.J. Mills and Y. Wang, *Phil. Mag.* **90**:405-436 (2010)



M. Fahrmann, W. Hermann, E. Fahrmann, A. Boegli, and T. Pollock, *Materials Science and Engineering*, A260, 212-221 (1999).

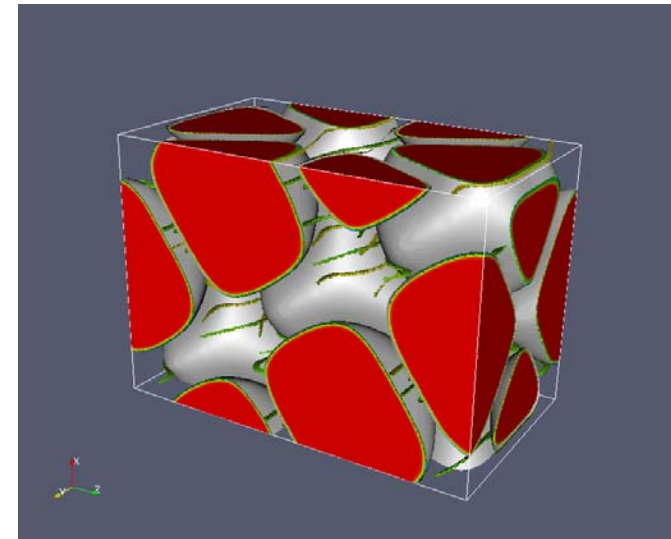
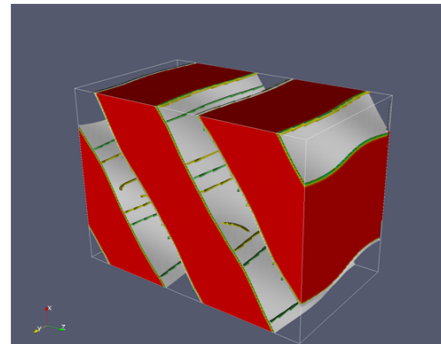
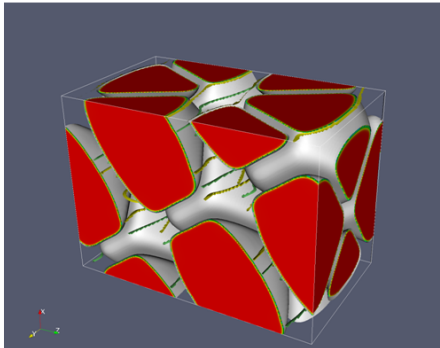
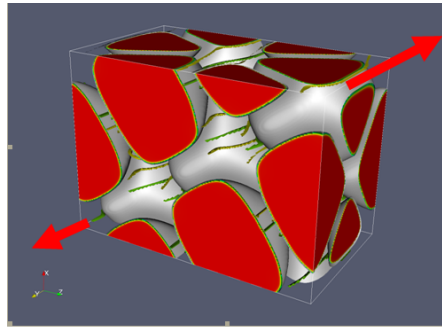
**To be quantitative:
(a) Operating mechanisms; (b) Material parameters**

Mechanisms of rafting



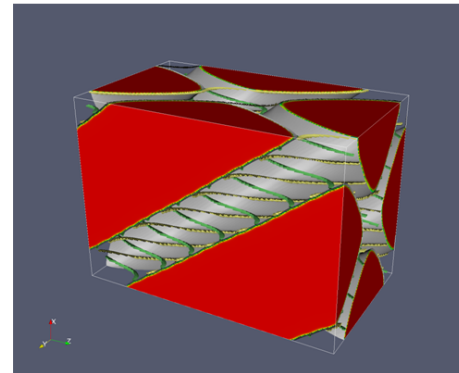
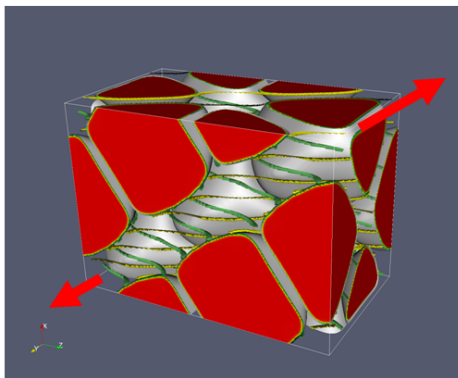
- Rafting caused by channel plasticity under homogeneous modulus assumption
- Rafting caused by modulus inhomogeneity without considering channel plasticity
- Rafting under combined effect of channel plasticity and modulus inhomogeneity

Dislocation level simulations



Time evolution of γ' particles in a Ni-Al alloy with **-0.3%** misfit under **152MPa** tensile stress along [001]. $D_{\text{eff}}=10^{-16}\text{m}^2/\text{s}$
 $t=3.6$ hrs; $t=7.2$ hrs; $t=10.7$ hrs.

Dislocations from different slip systems are represented by different colors



Modulus mismatch only ~ 50 hrs
 $(C_{11} - C_{12})^{\gamma} / (C_{11} - C_{12})^{\gamma'} = 85\%$

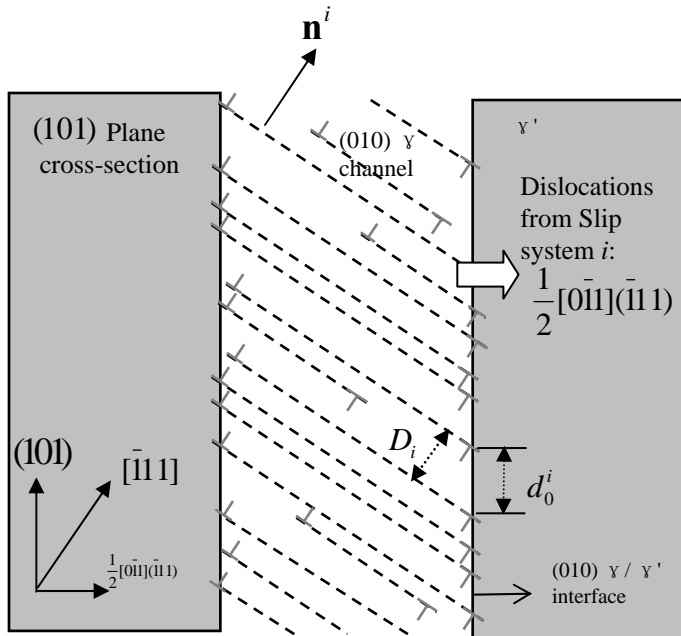
Channel plasticity only ~ 9 hrs

**Modulus mismatch +
Channel plasticity** ~ 7 hrs

Time evolution of γ' particles in a Ni-Al alloy with **+0.3%** misfit under **152MPa** tensile stress along [001].
 $t=3.6$ hrs; $t=7.2$ hrs.

N. Zhou et. al. Acta Mater. 55 (2007) 5369;
ibid 56 (2008) 6156.

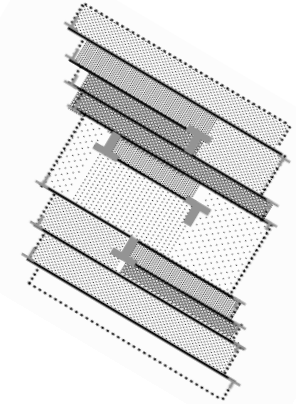
Local dislocation density approach



$$\eta_i(\mathbf{r}) = \frac{|\mathbf{b}^i|}{D_i(\mathbf{r})} \quad \text{Order parameter corresponds to local plastic strain}$$

$$\hat{\boldsymbol{\varepsilon}}^T(\mathbf{r}) = \sum_{i=1..12} \frac{(\mathbf{n}^i \otimes \mathbf{b}^i + \mathbf{b}^i \otimes \mathbf{n}^i)}{2|\mathbf{b}^i|} \cdot \eta_i(\mathbf{r})$$

$$d_0^i = \frac{\sqrt{6}}{2} D_i(\mathbf{r}) = \frac{\sqrt{6}}{2} \frac{|\mathbf{b}^i|}{\eta_i(\mathbf{r})}$$



$$F = \int_V dV \left\{ f(c(\mathbf{r}), \phi_p(\mathbf{r})) + \frac{K_\phi}{2} \sum_{p=1}^4 (\nabla \phi_p(\mathbf{r}))^2 \right\} + E^{grad-\eta} + E^{el}$$

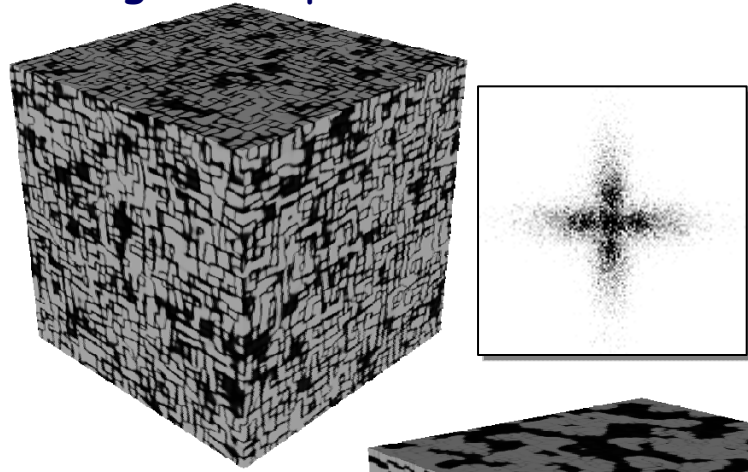
$$E^{grad-\eta} = \frac{\beta}{2} \int \sum_{i=1..8} [\mathbf{n}^i \times \nabla \eta_i(\mathbf{r})] \cdot [\mathbf{n}^i \times \nabla \eta_i(\mathbf{r})] d^3r$$

$$\frac{\partial c(\mathbf{r})}{\partial t} = \nabla \cdot \left\{ M_c \nabla \left[\frac{\delta F}{\delta c(\mathbf{r})} \right] \right\}$$

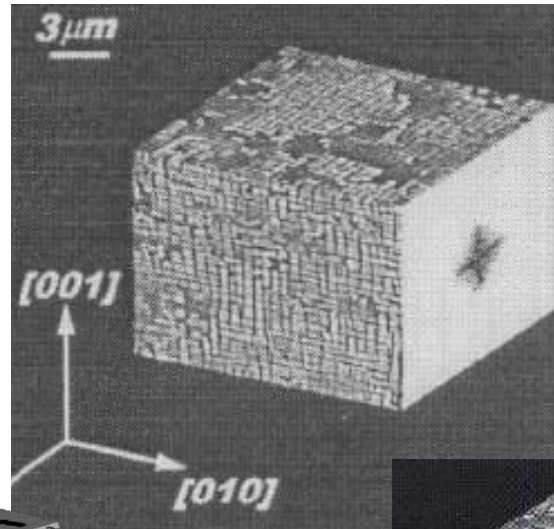
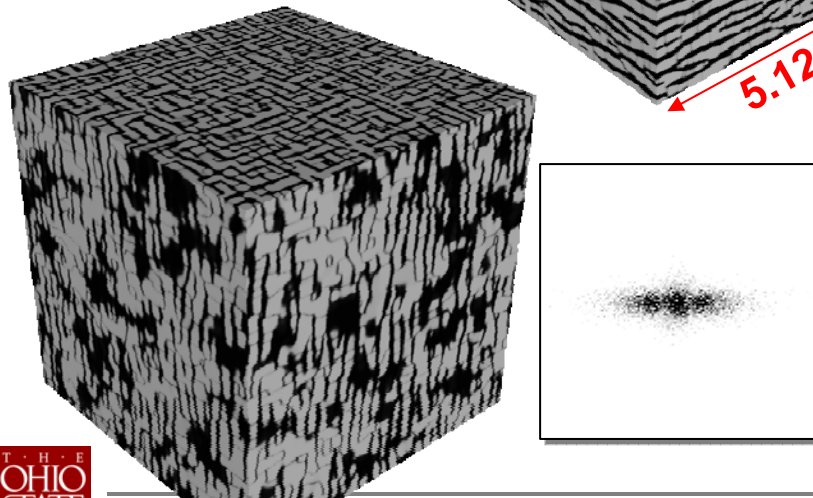
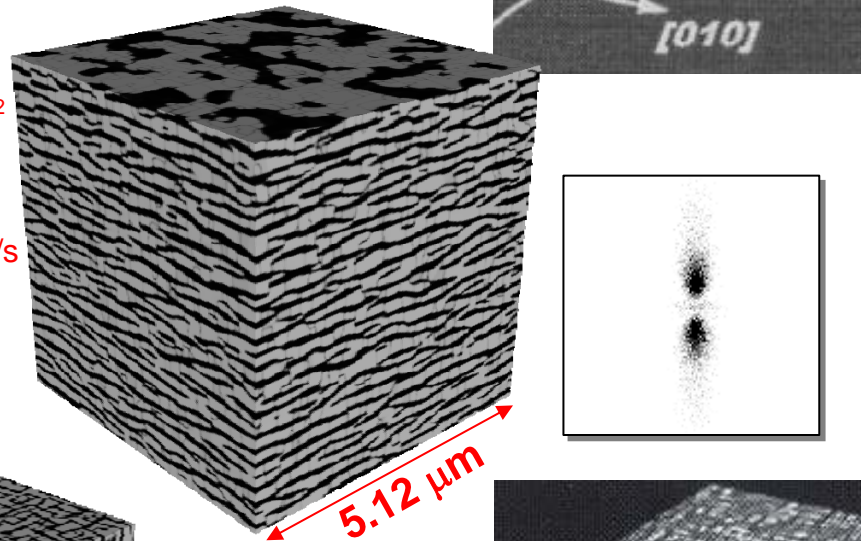
$$\frac{\partial \phi_p(\mathbf{r})}{\partial t} = -L_\phi \frac{\delta F}{\delta \phi_p(\mathbf{r})}$$

$$\frac{\partial \eta_i(\mathbf{r})}{\partial t} = -L_\eta \frac{\delta F}{\delta \eta_i(\mathbf{r})}$$

Coarse-grained phase field simulations

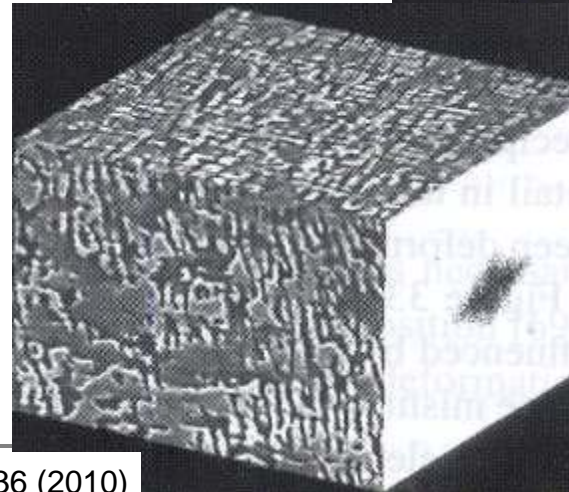
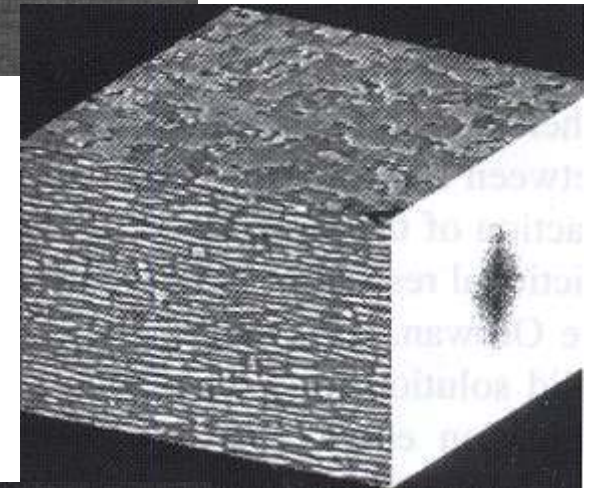


Interfacial energy: 14 mJ/m²
 Applied stress: 152Mpa
 Temperature: 1300K
 Effective diffusivity: 10⁻¹⁶m²/s
 Volume fraction of γ' : 60%
 Lattice misfit: -0.3%
 Aging time: 5.67 hours



Experimental observations

Misfit: -0.5%
 Applied stress: 130MPa
 Temperature: 1050°C
 Aging time: 8 hrs.

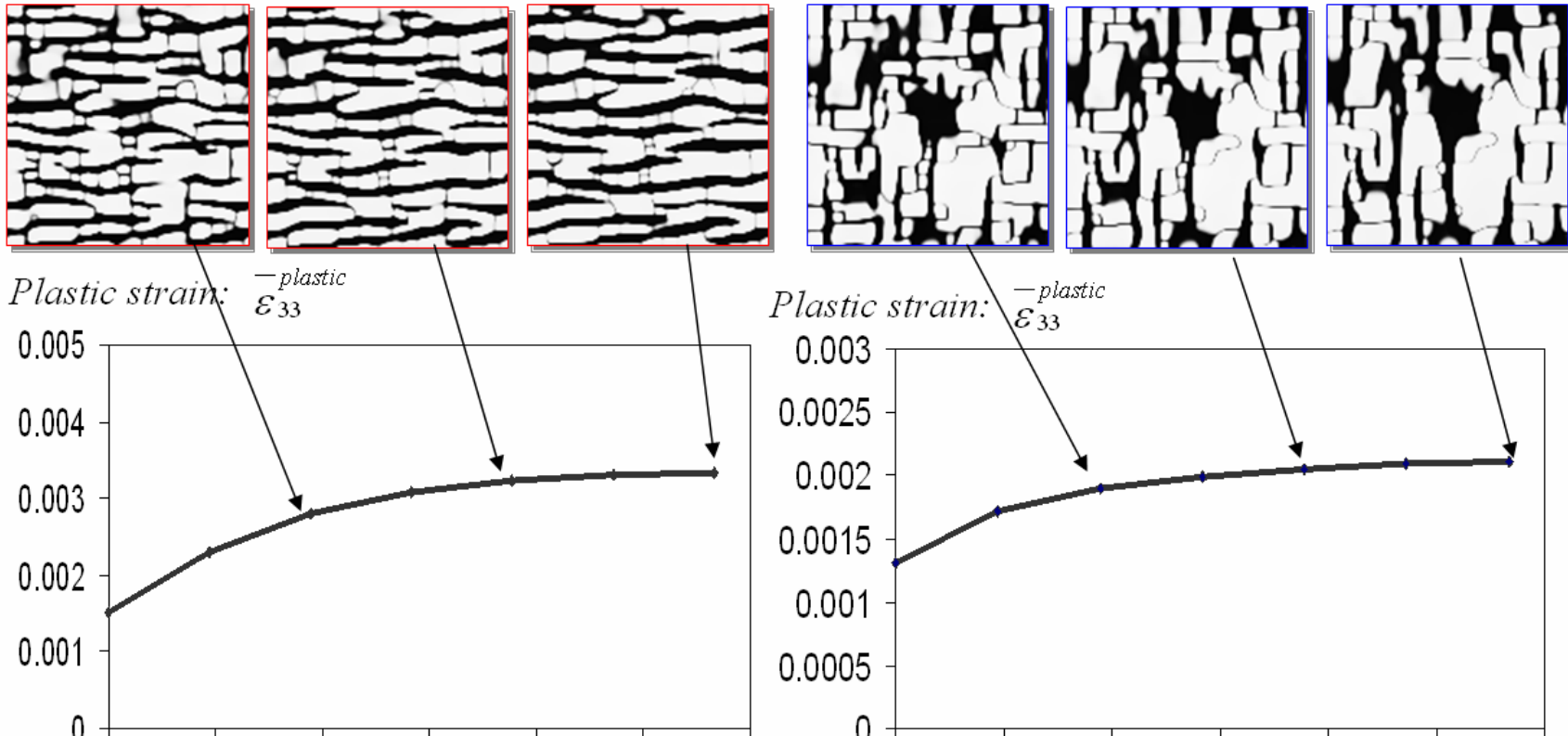


M. Fahrman, W. Hermann, E. Fahrman, A. Boegli, and T. Pollock, *Materials Science and Engineering*, A260, 212–221 (1999).



Creep strain vs. time

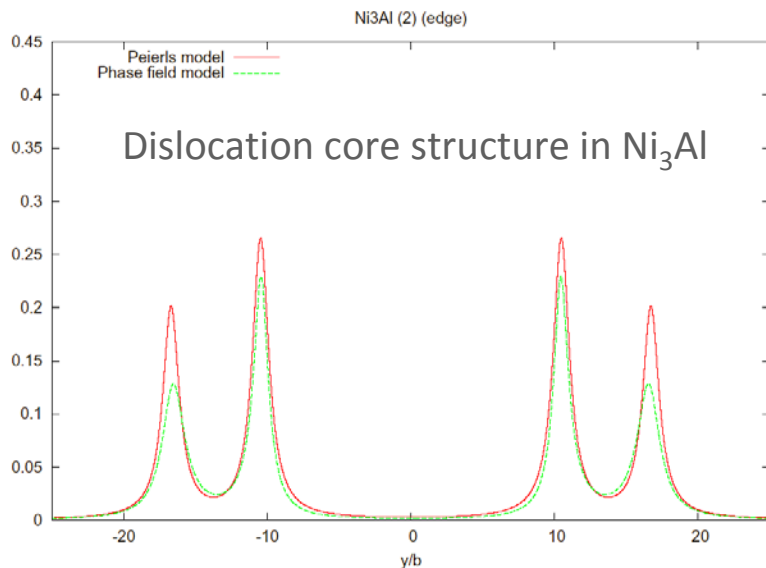
(100) Plane cross-section during rafting process



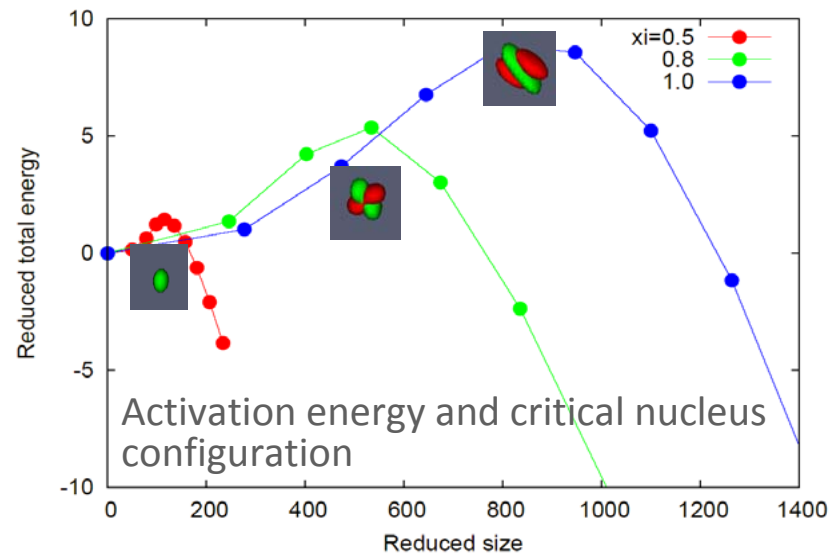
The coarse-grained model could be used in the optimization of existing alloys and development of new alloys such as Co-base superalloys if properly informed and validated.

II. Microscopic Phase Field Model

- Works at natural length scales of extended defects (\sim nm)
- Using DFT calculations of *GSF/MGSF* and Landau free energy as direct inputs and **predict defect structure, chemistry and energy**
- Probe the total energy landscape using NEB for **saddle point configuration and activation energy of defect nucleation**
- When combined with experimental characterization, it could serve as a powerful tool to explore **deformation/transformation mechanisms** and provide critical inputs to coarse-grained phase field simulations



Wang and Li, Acta Mater, Overview 150, 2010



Shen. et. al. Met. Trans. 39A:976 (2008)

II. Microscopic Phase Field Model (Cont.)

Reprinted from THE JOURNAL OF CHEMICAL PHYSICS, Vol. 28, No. 2, 258–267, February, 1958
Printed in U. S. A.

Free Energy of a Nonuniform System. I. Interfacial Free Energy

JOHN W. CAHN AND JOHN E. HILLIARD
General Electric Research Laboratory, Schenectady, New York
(Received July 29, 1957)

Reprinted from the JOURNAL OF CHEMICAL PHYSICS, Vol. 31, No. 3, 688–699, September, 1959
Printed in U. S. A.

Free Energy of a Nonuniform System. III. Nucleation in a Two-Component Incompressible Fluid

JOHN W. CAHN AND JOHN E. HILLIARD
General Electric Research Laboratory, Schenectady, New York
(Received February 16, 1959)

Comment by Mullins: The fundamental properties associated with an interface and a critical nucleus are expressed in terms of the parameters in the free energy model and there is no need to introduce the artificial dividing surface of Gibbs, nor to define a separate interfacial energy, nor to model the nucleus as homogeneous

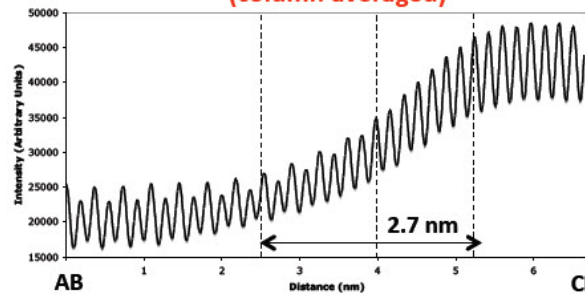
Defect cores are diffuse at their natural length scales



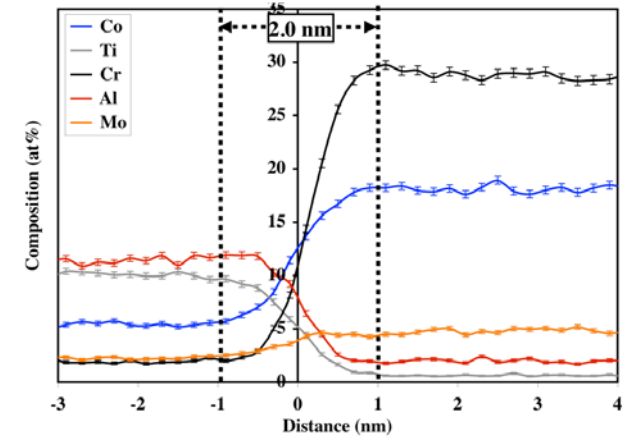
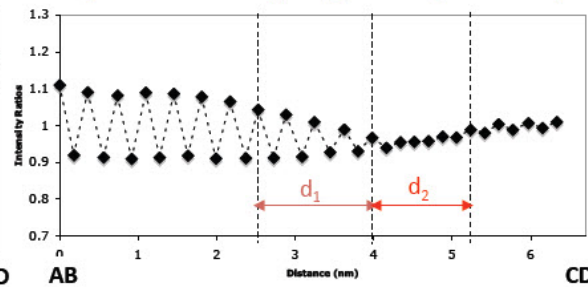
HRSTEM

3D atom probe

Intensity Profile across interface
(column averaged)

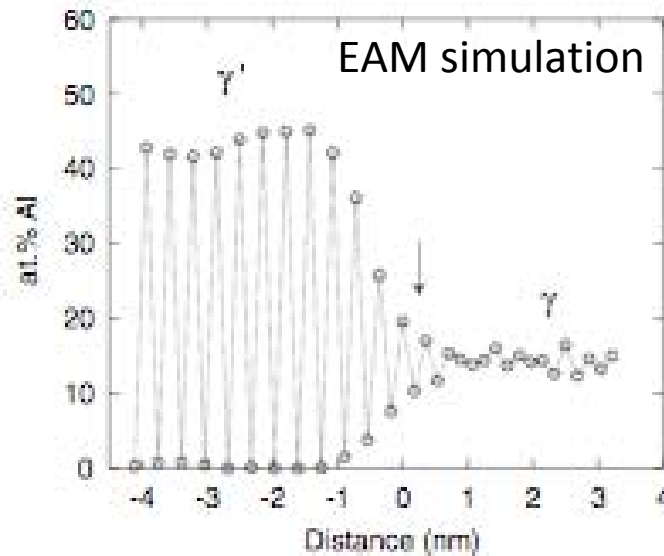


Ratio of Alternate Column Intensities
(measure of long-range order parameter)



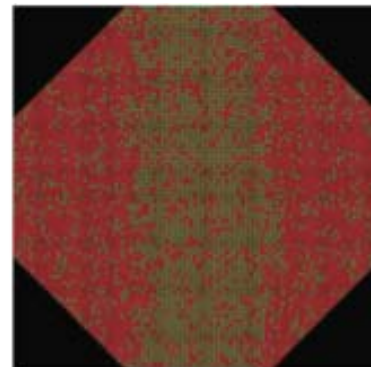
Srinivasan et. al. Phys. Rev. Lett. (2009)

EAM simulation

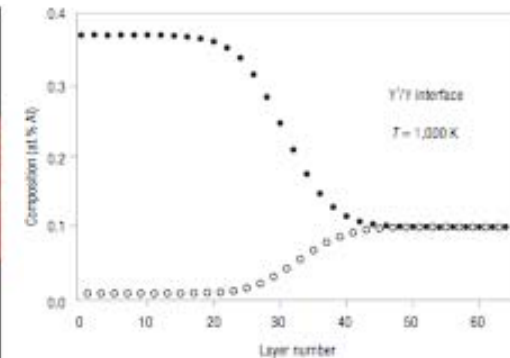


Y. Mishin, *Acta Materialia*, 52 (2004), 1451

Order-disorder transition ~ 6-8 planes



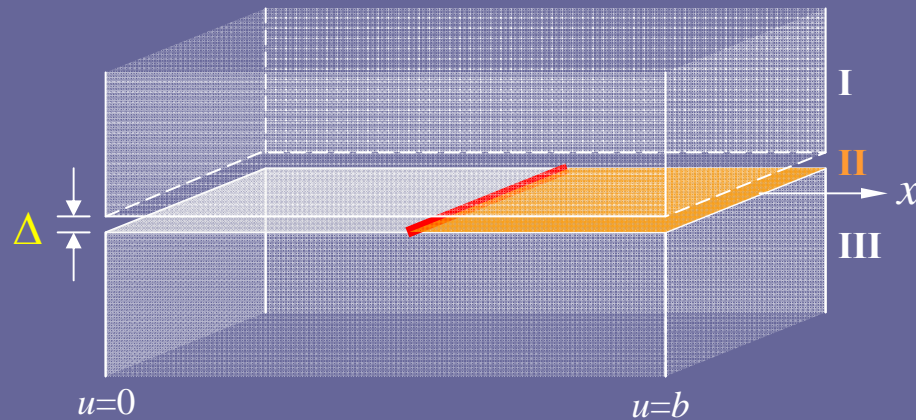
Monte Carlo simulation



A.J. Ardell, V. Ozolins, *Nature Materials*, 4 (2005) 309

Order-disorder transition ~ 10 planes

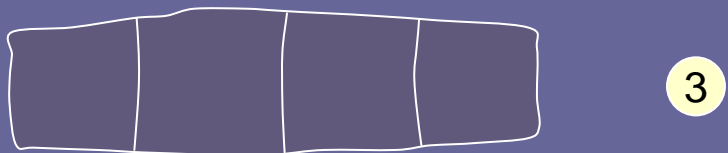
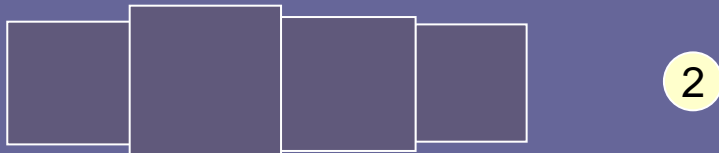
Microscopic phase field model vs. Peierls model



$$\sigma(x) = 2\tilde{H} \int_{-\infty}^{+\infty} \frac{\partial u(s)}{\partial s} \frac{1}{x-s} ds \quad (\text{elastic})$$

$$f(x) = -\frac{\mu b}{2\pi d} \sin \frac{2\pi u(x)}{b} \quad (\text{inelastic})$$

$$a = a(\phi)$$



$$F = \int [f(\phi(\mathbf{r})) + \kappa |\nabla \phi(\mathbf{r})|^2] d\mathbf{r} + E_{el}$$

1
2
3

(inelastic)

(elastic)

Microscopic phase field model vs. Peierls model

$E^{elast}[\eta]$ — The phase field microelasticity formulation is a superset of the Peierls model. Instead of $\log(r)$ type dislocation line-to-line interaction kernel, it employs $1/r$ type voxel-to-voxel interaction kernel.

$E^{cryst}[\eta]$ — Crystalline energy – 3D generalization of the misfit energy. It is a potential energy landscape subject to a general plastic strain produced by an arbitrary linear combination of slips (localized simple shears). It reduces to GSF energy when projected onto a particular slip plane.

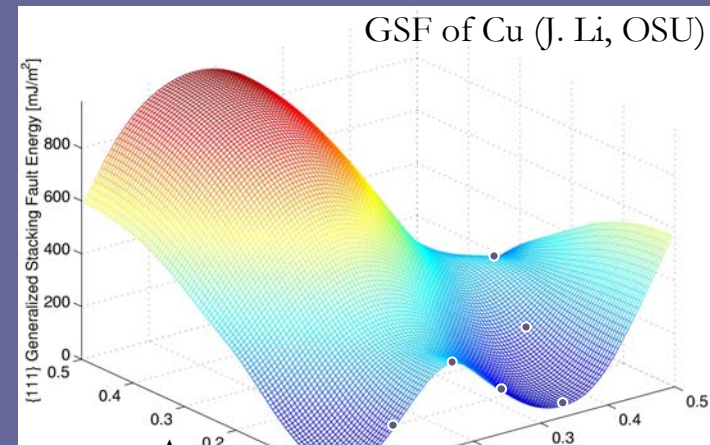
$$E^{cryst} = \int d\mathbf{r} \phi(\boldsymbol{\varepsilon}^s(\mathbf{r}))$$

Inter-planar potential:

$$\phi(\boldsymbol{\varepsilon}^s) \rightarrow \gamma(\mathbf{b})/d$$

Shen & Wang, Acta Mater

51(2003)2595

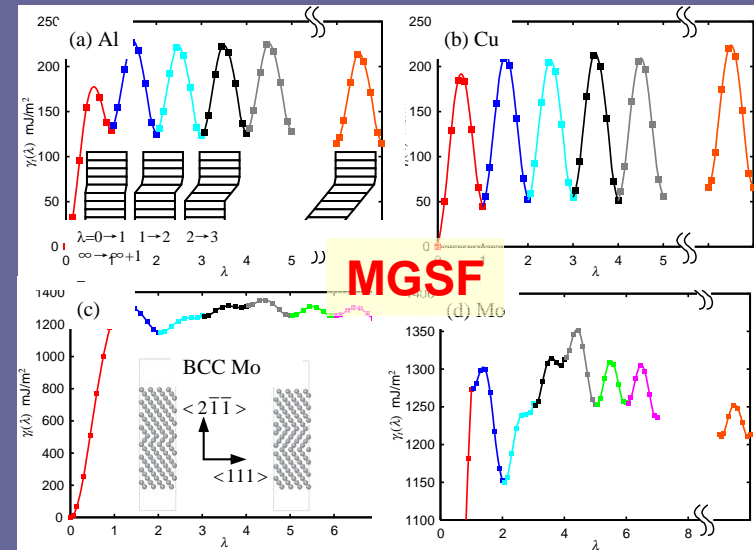
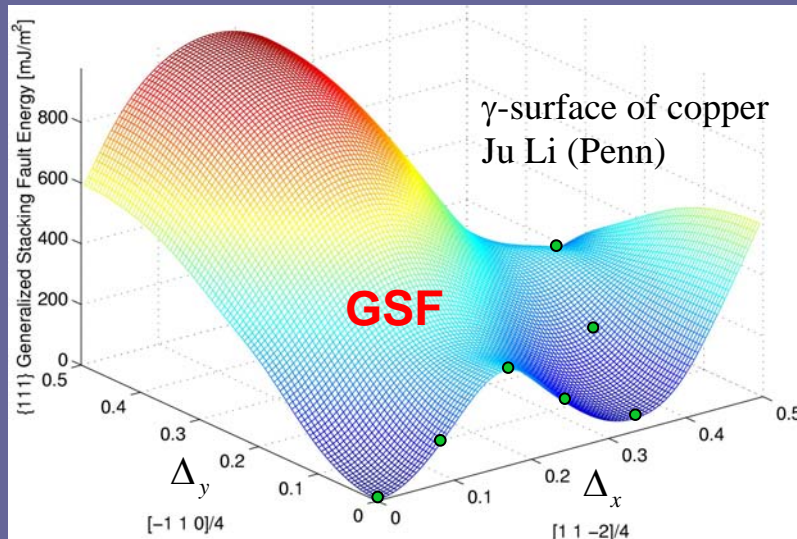


Phase field approach is a superset of the Cahn-Hilliard description of chemical non-uniformities and the Peierls description of displacive non-uniformities.

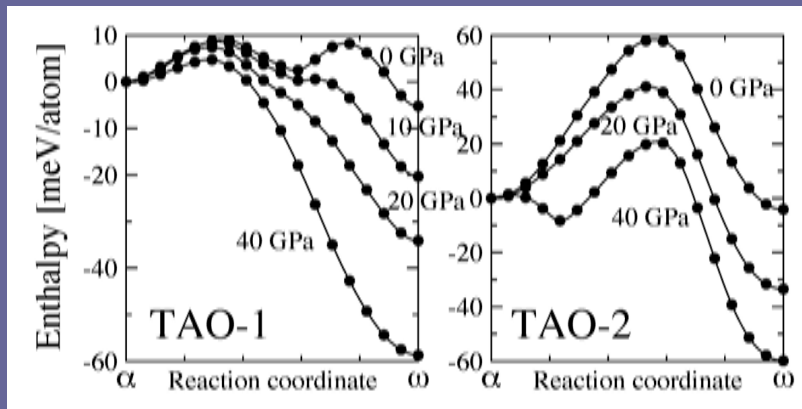
Gradient energy term offers additional degree of freedom to
 approximation of the P-N model (see S. Wang, Phys. Rev. B 65:094114)

Wang an Li, Acta Mater, Overview 150, 2010

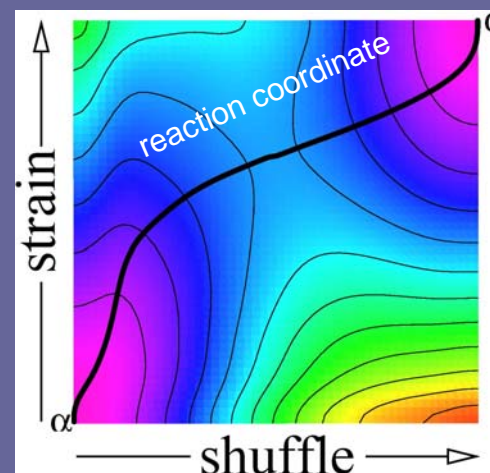
Energy landscape calculation by *ab initio*



GSF energy for dislocation core structure/energy, peierls stress, nucleation barrier
MGSF energy for twin nucleation and growth



$\alpha \rightarrow \omega$ transformation in Ti

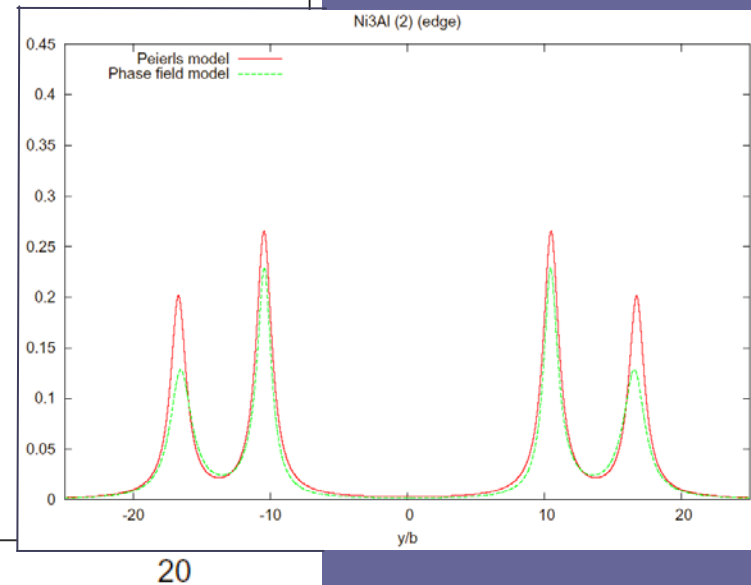
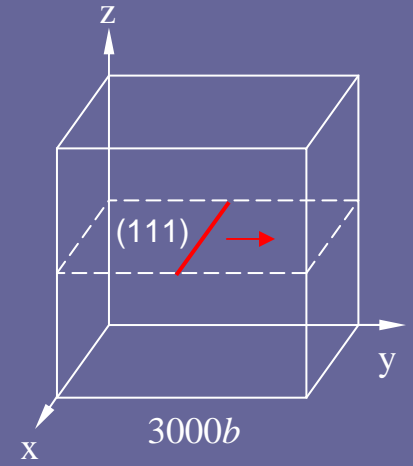
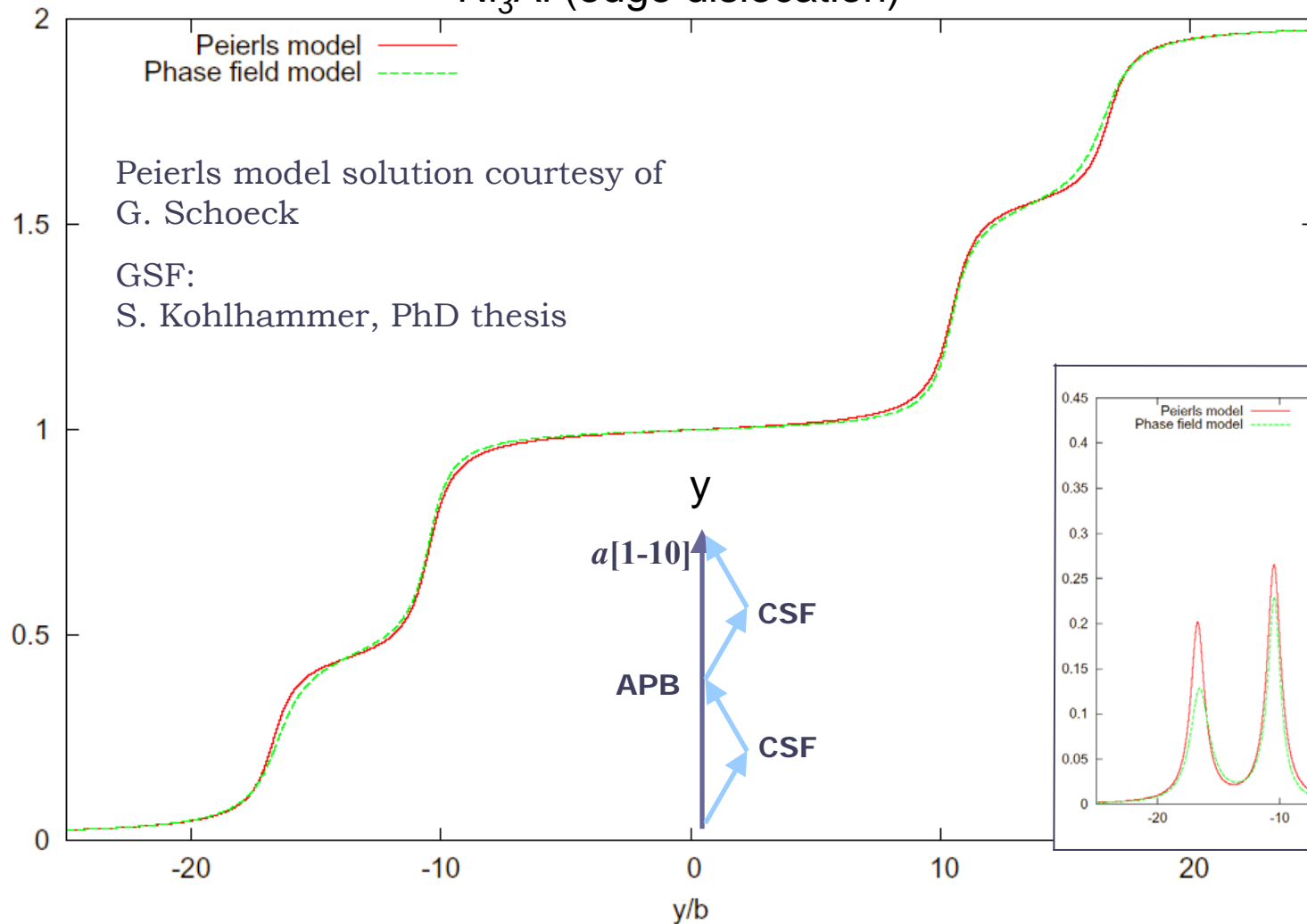


(Trinkle et. al. PRL 2003)

Landau free energy
 for martensitic
 transformation -
 “MGSF” energy for
 martensite nucleation
 and growth

Dislocation core structure (disregistry)

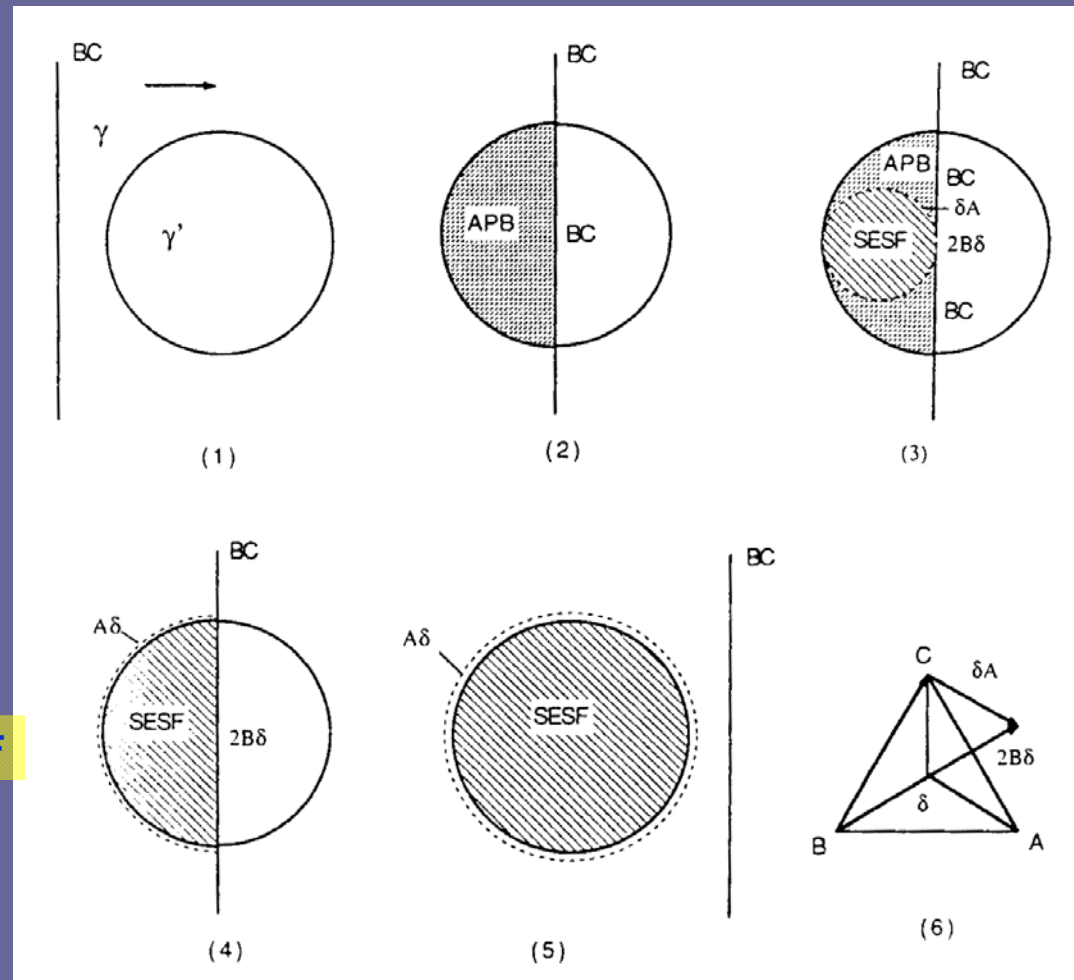
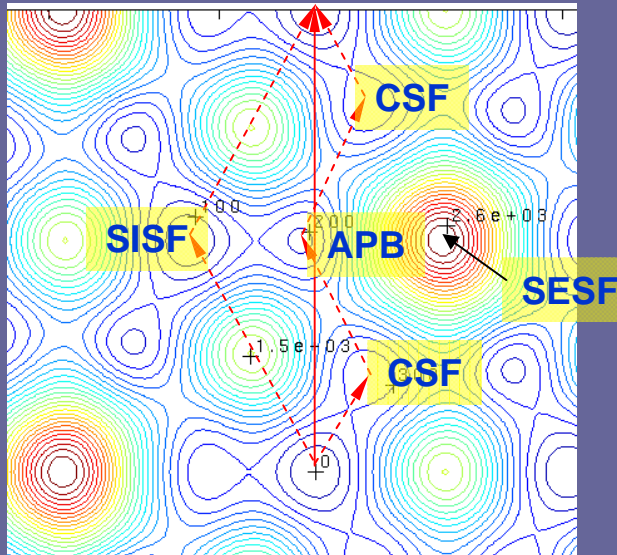
Ni₃Al (edge dislocation)



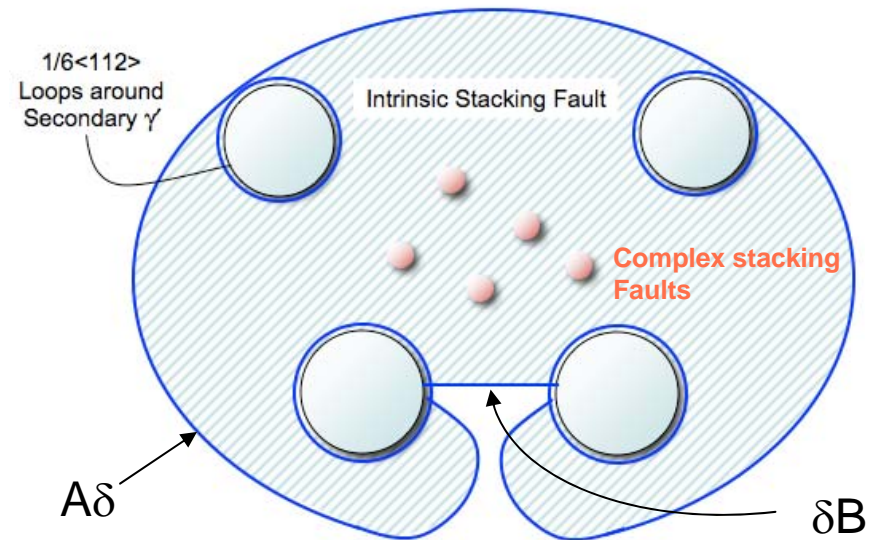
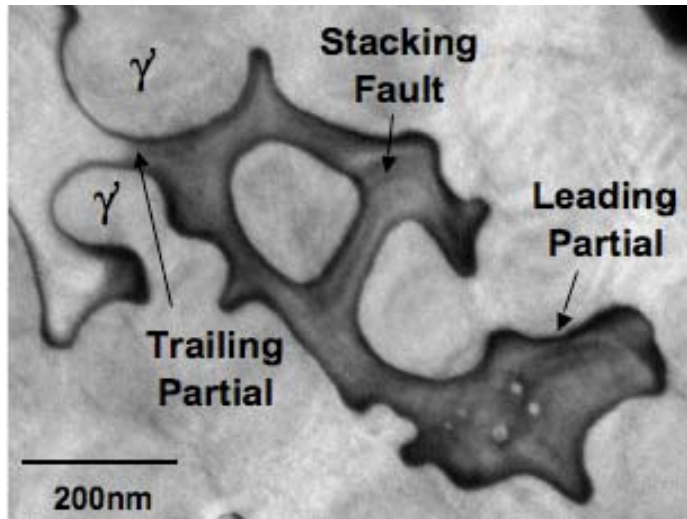
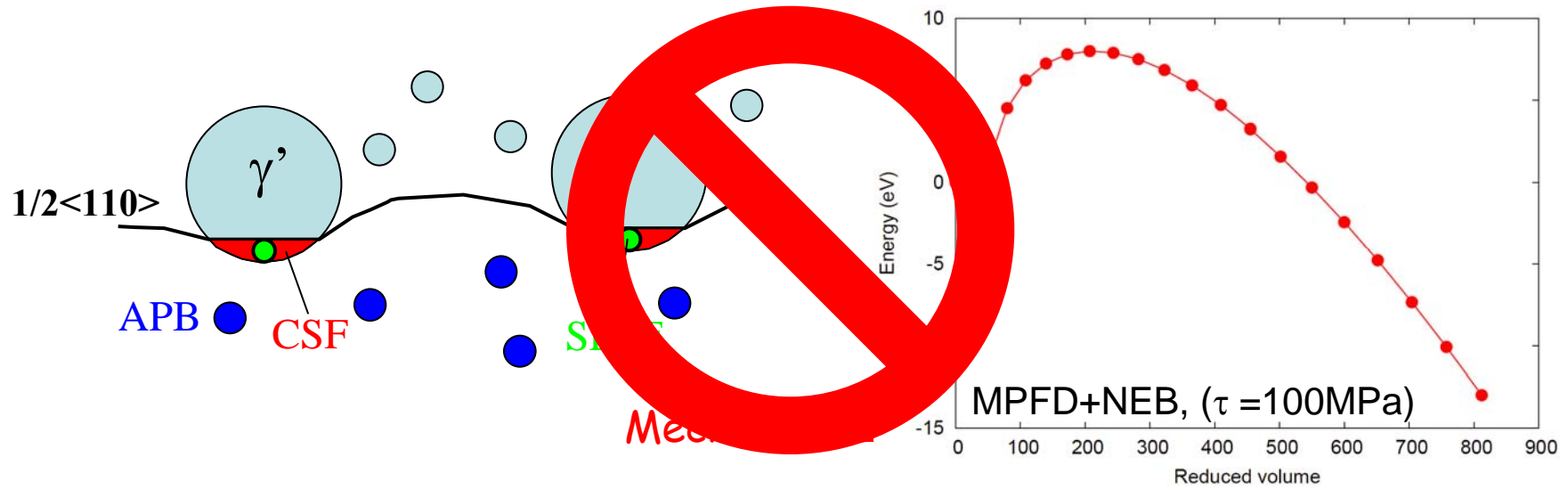
Micromechanisms of γ' shearing

Model proposed by Decamps et. al. (1987, 1991, 1994) and Mukherji et. al. (1991):

- Precipitate sheared initially by $1/2\langle 110 \rangle$ forming an APB
- APB transforms into SISF/SESF via nucleation on APB of $1/6\langle 112 \rangle$ partial

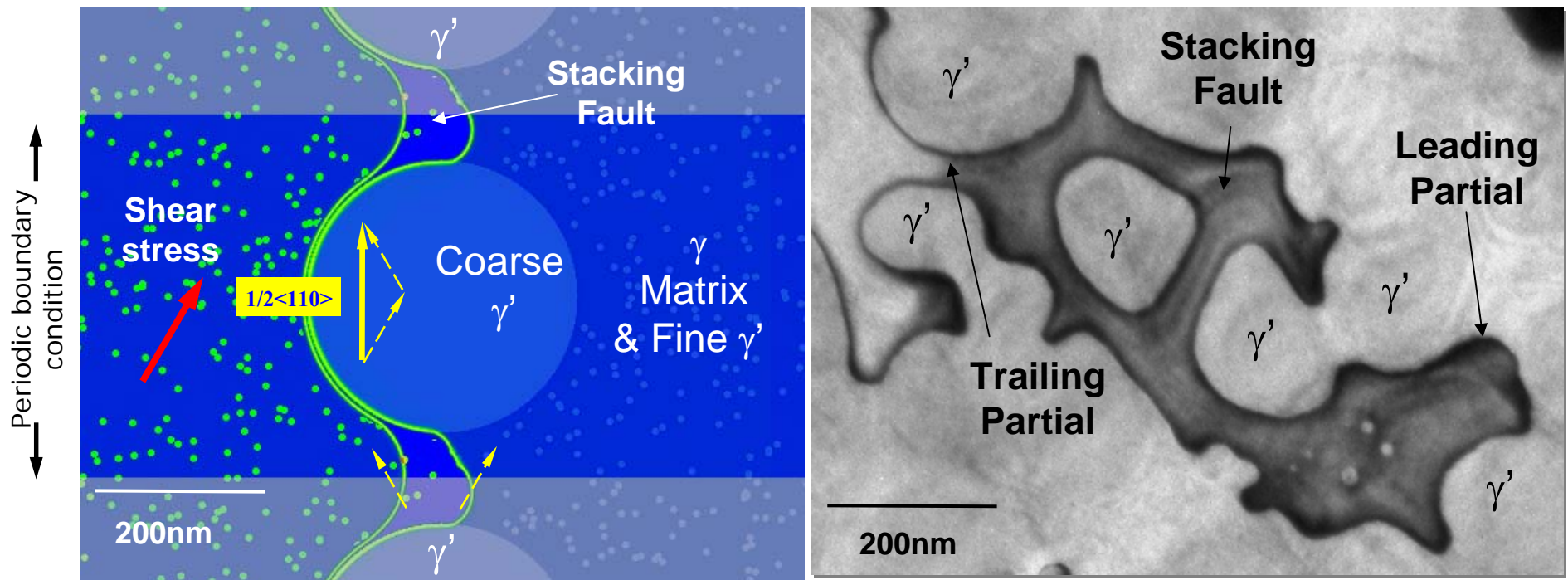


MPF exploration of possible mechanisms



Mechanism II

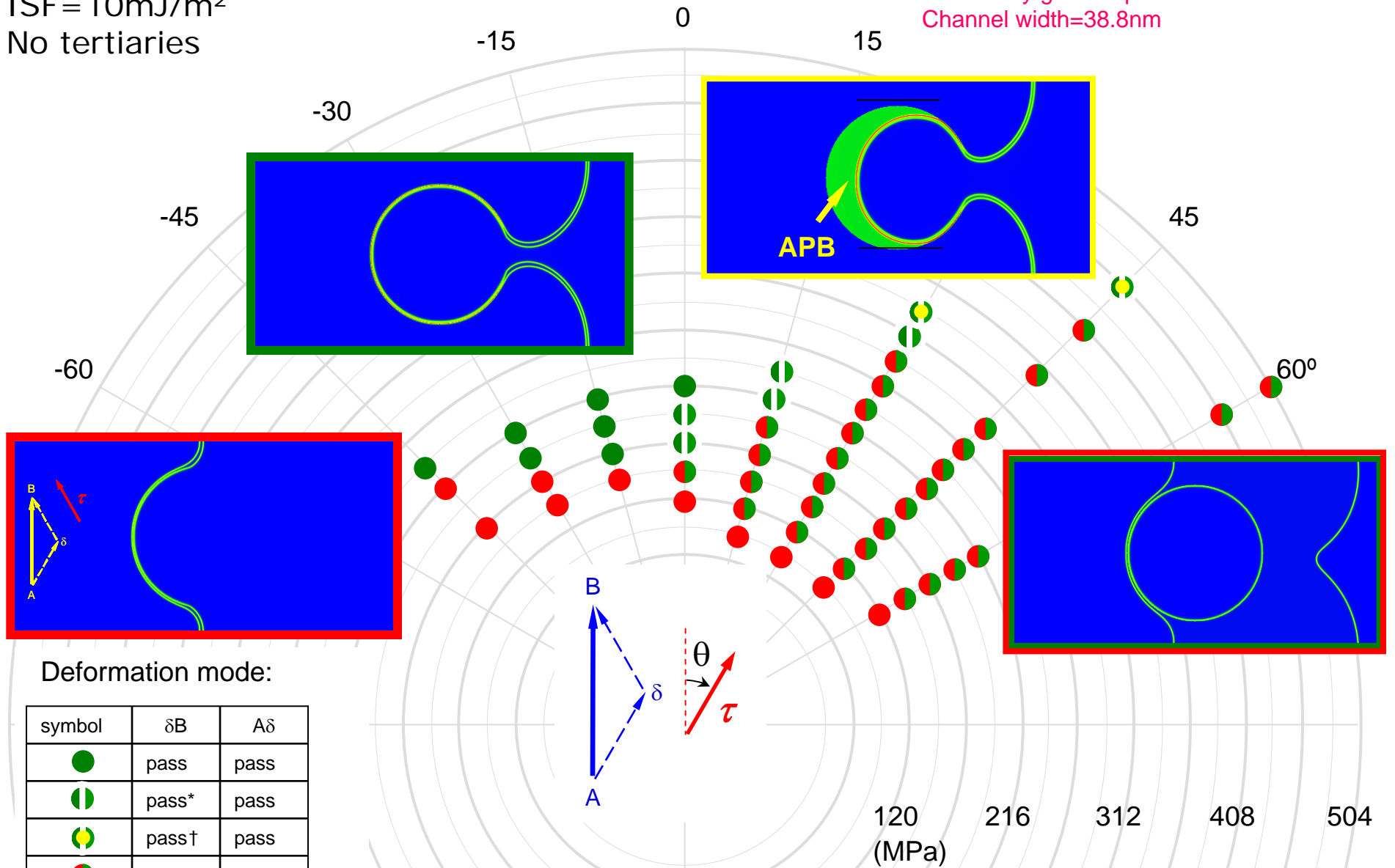
Decorrelation of Shockley partials



- Use simulations to parametrically study behavior as function of:
 - Secondary and tertiary size and volume fraction → **“Microstructure”**
 - Matrix stacking fault energy |→ **“Chemistry”**
 - Precipitate stacking fault energies |→ **“Chemistry”**
 - Applied shear stress |→ **“Loading”**
 - Applied shear stress orientation |→ **“Loading”**

ISF = 10 mJ/m²
 No tertiaries

Secondary gamma prime diameter = 233 nm
 Channel width = 38.8 nm

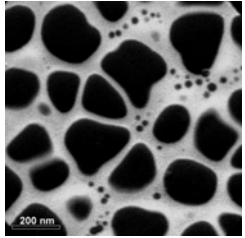


Deformation mode:

symbol	δB	$A\delta$
●	pass	pass
◐	pass*	pass
◑	pass†	pass
◒	stop	pass
●	stop	stop

* de-correlated
 † form APB

- Intricate orientation dependence
- Decorrelation for favorable orientations at low stress



Experimental image as direct input

From Ray Unocic

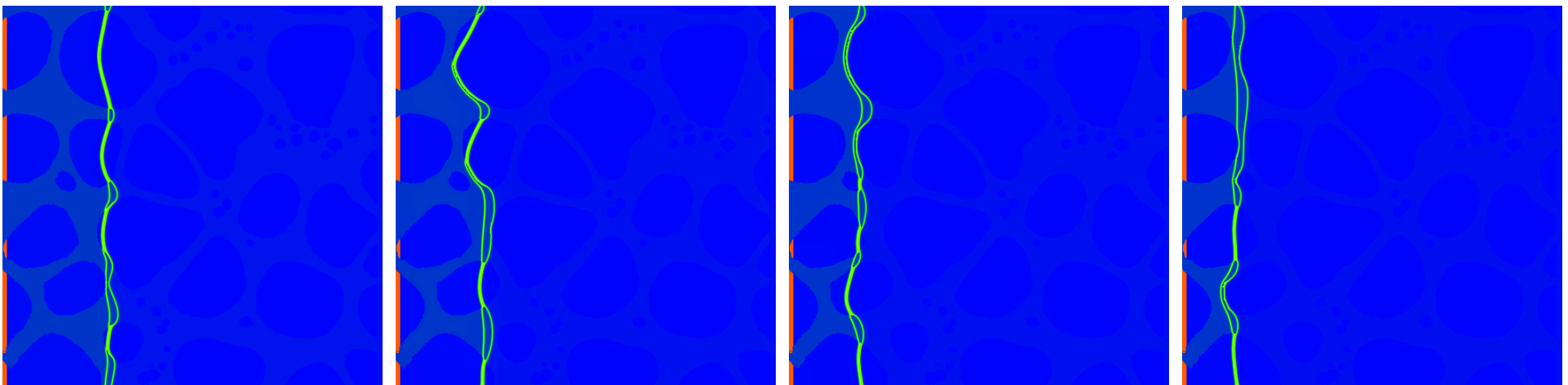
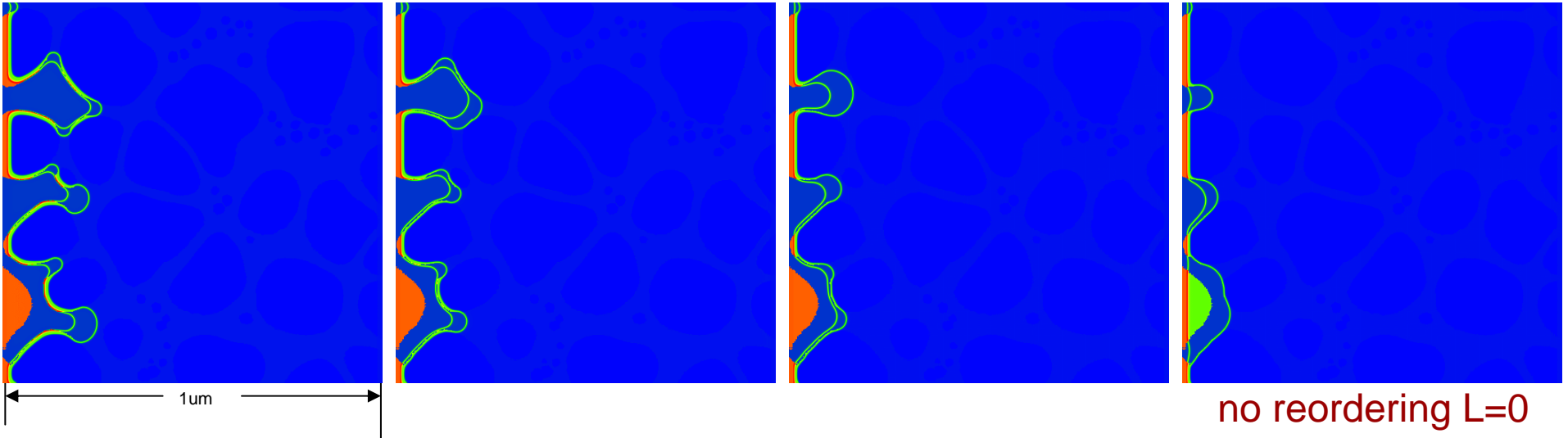
Parametric study of SESF shearing

1000MPa

800MPa

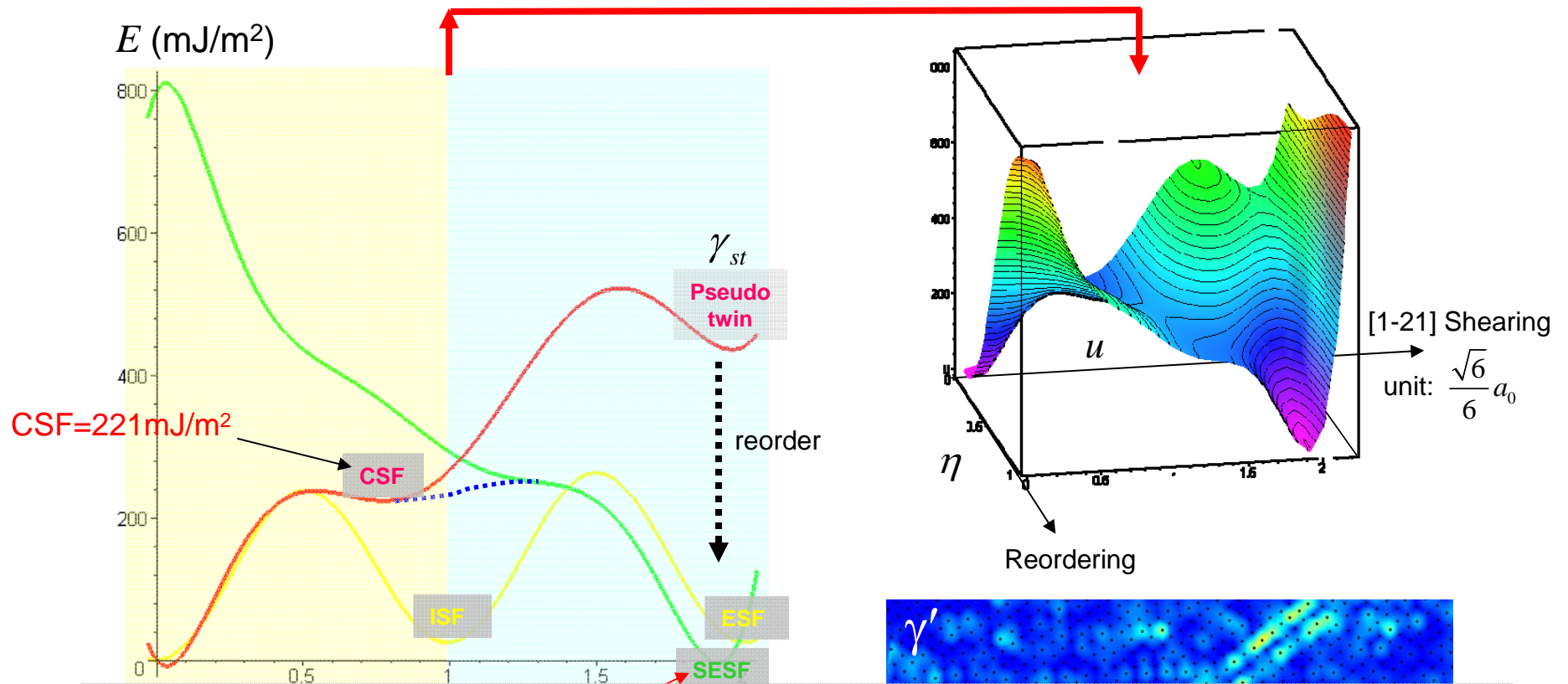
600MPa

400MPa



with reordering: $L=5$

Chemical – mechanical coupling



To develop such a free energy landscape, new modeling capabilities are required that can describe diffusion-controlled defect migration and microstructural evolution with resolution at the cores of the interacting defects - Diffusive MD

Conclusions

Microstructure evolution in solids often involves coupled displacive/diffusional process as a rule rather than as an exception. The phase field approach is well suited to treat such complexities in an integrated manner.

But major advances have to be made before transforming the approach to **quantitative and material specific tools**

- Direct utilization of *ab initio* energetics and interatomic potentials (DMD)
- Formulation of Landau free energy along the reaction-coordinate
- Identification and incorporation of deformation/transformation mechanisms, in combination with experimental characterization
- Integrating phase field techniques at different length scales (DMD, MPF and CGPF).